Ceramics International 45 (2019) 9231–9244

Contents lists available at ScienceDirect

Ceramics International

journal homepage: www.elsevier.com/locate/ceramint

Cation-doped bioactive ceramics: *In vitro* bioactivity and effect against bacteria of the oral cavity

Renato Luiz Siqueira[a,b,*], Patrícia Francieli Silva Alves[c], Thaís da Silva Moraes[c], Luciana Assirati Casemiro[c], Sidney Nicodemos da Silva[b], Oscar Peitl[a], Carlos Henrique Gomes Martins[c], Edgar Dutra Zanotto[a]

[a] Laboratório de Materiais Vítreos, Departamento de Engenharia de Materiais, Universidade Federal de São Carlos, Rodovia Washington Luís km 235, 13565-905, São Carlos, SP, Brazil
[b] Departamento de Engenharia de Materiais, Centro Federal de Educação Tecnológica de Minas Gerais, Avenida Amazonas 5253, 30421-169, Belo Horizonte, MG, Brazil
[c] Laboratório de Pesquisa em Microbiologia Aplicada, Universidade de Franca, Avenida Doutor Armando de Sales Oliveira 201 — Parque Universitário, 14404-600, Franca, SP, Brazil

ARTICLE INFO

Keywords:
Solid-state reaction
Bioactive ceramic
Bioactivity test
Antibacterial activity

ABSTRACT

We synthesized, using a solid-state reaction, bioactive ceramics of the $SiO_2-CaO-Na_2O-P_2O_5$ system doped with up to 3 mol% of Ag, Mg, Sr, Zn, and Ga, elements that were used as therapeutic agents. On evaluating the *in vitro* bioactivity of our crystalline samples using the ICG-TC04 method (so far only tested for glassy materials), we observed that those ceramics containing up to 0.5 mol% dopant exhibited hydroxycarbonate apatite (HCA) layer formation on their surfaces in a 24-h *in vitro* assay — the same time observed for Bioglass®, the material considered to be "gold standard" in terms of bioactivity. The antibacterial activity of these ceramics was confirmed against 23 oral bacteria, related to caries and endodontic infections, by employing three different methods. For the agar dilution method, using a concentration range of 0.5–24 mg/mL, various bacteria were found to be susceptible to the materials — the lowest minimum inhibitory concentration (MIC) values were achieved for the doped samples, particularly those containing Ag. In the biofilm-forming capability assay, we did not observe any viable cells after 24 h incubation. Finally, the direct contact assay confirmed that all the samples showed a stronger antibacterial effect, promoting a significant reduction in the number of viable cells after only 10 min in contact with the microorganisms. This result indicates that the tested materials have an intrinsic antibacterial activity, and do not need to be doped, except for some specific bacteria or depending on how they will be used (extracts or in direct contact). Therefore, besides easy production and *in vitro* bioactivity, all tested materials demonstrated a considerable antibacterial effect against representative bacteria, stimulating future studies involving their application as topical endodontic disinfectants or in dental prophylaxis procedures.

1. Introduction

Bioactive ceramics are materials that rapidly (in a few hours or days) bond with hard tissues and some soft tissues, stimulating bone growth away from the bone-implant interface [1]. The first synthetic material that exhibited this level of interaction was the 45S5 $45SiO_2-24.5CaO-24.5Na_2O-6P_2O_5$ (wt%) glass, known worldwide for its trademark Bioglass® [2]. Today, it is known that other materials, such as novel glass types, glass-ceramics, and calcium phosphate-based ceramics also exhibit high bioactivity [1–3] (i.e., the ability to form *in vivo* a hydroxycarbonate apatite (HCA) layer on their surfaces, promoting an interface and strong bonds to bone and teeth). It is important to note that applications of these materials are not restricted to hard tissue (bone and teeth). Numerous soft tissue engineering applications have been investigated recently [4], most with exciting potential, including cardiac tissue, nerve and gastrointestinal regeneration, stabilization of percutaneous devices, and anchoring of ligament prostheses.

To further improve the performance of bioactive ceramics, new approaches have been investigated by incorporation of biologically active ions in their structures [5,6]. The main objective has been to

* Corresponding author. Laboratório de Materiais Vítreos, Departamento de Engenharia de Materiais, Universidade Federal de São Carlos, Rodovia Washington Luís km 235, 13565-905, São Carlos, SP, Brazil.
E-mail address: rastosfix@gmail.com (R.L. Siqueira).
URL: http://www.certev.ufscar.br (R.L. Siqueira).

https://doi.org/10.1016/j.ceramint.2019.02.001
Received 6 January 2019; Accepted 1 February 2019
Available online 08 February 2019

increase the stimulating effects of these materials on osteogenesis or angiogenesis, and for promoting antimicrobial activity. Regarding antimicrobial activity (the focus of this article), it has been reported that some materials, such as S53P4 $53SiO_2 - 20CaO - 23Na_2O - 4P_2O_5$ (wt %) glass [7,8], Bioglass® [9,10] and certain gel-glasses [11,12], exhibit this property. As an example, S53P4 glass demonstrated potential to treat osteomyelitis [13–15], an inflammatory process of bone tissue that is very difficult to eradicate, particularly when associated with the presence of *Staphylococcus aureus* and *S. epidermidis* biofilms.

In addition to the fact that some bioactive ceramics present antimicrobial activity, it is possible to intensify this effect by incorporation of certain ions in their structure. Silver, for example, has broad spectrum antimicrobial activity [16,17], and glasses containing this element have been synthesized using different techniques [18–20]. Hence, these materials have been pointed out as a promising alternatives for tissue engineering applications, especially in cases involving healing of cutaneous wounds [21,22]. Gallium is another element that has attracted significant interest in recent years. *In vitro* studies have shown that Ga^{3+} is effective in inhibiting the formation and growth of *Pseudomonas aeruginosa* biofilms due to its chemical similarity to Fe^{3+} [23], thus interfering in the cellular metabolism of this bacterium, which has an intrinsic resistance against antibiotics and is responsible for numerous cases of hospital infection. The incorporation of only 1 mol% Ga_2O_3 into phosphate glasses was sufficient to promote a positive effect against *P. aeruginosa*, *S. aureus*, methicillin-resistant *S. aureus*, *Escherichia coli*, and *Clostridium difficile* [24]. It is important to emphasize that, besides having antibacterial activity, gallium also has a biological action favorable to the maintenance of bone tissue [25]. It acts by inhibiting the process of bone resorption, therefore being suggested as a promising agent in the nonhormonal treatment of osteoporosis [26], somewhat similar to strontium [27–29].

It is remarkable how the incorporation of silver, gallium, and other biologically active elements in bioactive glasses, glass-ceramics, and ceramics, to enhance or give them new functionalities, is a promising and sound area of research. Beyond encompassing new compositions and synthesis methodologies, there have also been continuous efforts towards understanding the biological behavior of these materials, a process which is fundamental to direct modifications aiming at more specific and efficient applications. Hereupon, in this study, we evaluated the *in vitro* bioactivity and antibacterial activity of silica-based bioactive ceramics containing up to 3 mol% of silver (Ag), magnesium (Mg), strontium (Sr), zinc (Zn), and gallium (Ga) against potentially pathogenic bacteria of the oral cavity. Our purpose was to test the new ICG-TC04 method [30] to evaluate the *in vitro* bioactivity of crystalline materials. In addition, we intended to validate or not the antibacterial activity of these materials, which will help in the design of new applications — considering that resistance to antibiotics by some microorganisms, and the potential role of some dental lesions or periodontitis, as a risk factors for systemic diseases, indicate a clear demand for further strategies and alternatives for prevention and treatment.

2. Materials and methods

2.1. Bioactive ceramics

The bioactive ceramics evaluated in this research (Fig. 1) were synthesized using a solid-state reaction, following our previous study [31]. Thermal treatments for 480 min at ~1000 °C under a pure oxygen atmosphere were also tested here, mainly for the samples containing Ag. For the synthesis procedure, we used sodium carbonate ($Na_2CO_3 \geq 99.5\%$), calcium carbonate ($CaCO_3 \geq 99.5\%$), strontium carbonate ($SrCO_3 \geq 99.9\%$), disodium hydrogen phosphate ($Na_2HPO_4 \geq 99.5\%$), silver sulfate ($Ag_2SO_4 \geq 99.5\%$), silicon ($SiO_2 \geq 99.9\%$), magnesium ($MgO \geq 99.9\%$), zinc ($ZnO \geq 99.0\%$), and gallium ($Ga_2O_3 \geq 99.9\%$) oxides to achieve the nominal compositions shown in Table 1 — all chemicals were provided by Sigma-Aldrich. To obtain 50 g of material, the relative proportions of each chemical in the batch were calculated using the freely available software tool *GlassPanacea*® [32,33], allowing this step to be fast and accurate. For comparison, samples of Bioglass® and Biosilicate® were used as references. Biosilicate® is a bioactive glass-ceramic that is approximately 99.5% crystalline [34,35], and which has also been tested successfully in several medical and dental applications [36,37]. Both materials were provided by researchers of the Vitreous Materials Laboratory of the Materials Engineering Department at the Federal University of São Carlos, Brazil.

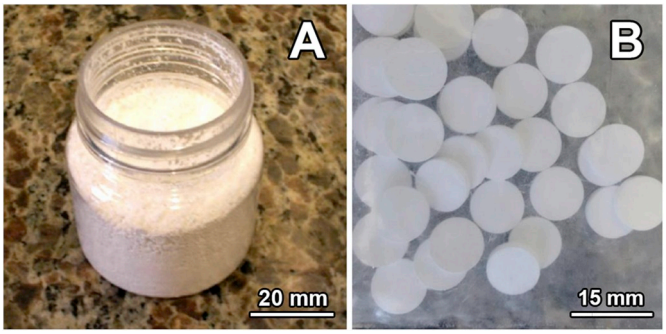

Fig. 1. Illustration of a sample evaluated in the study: a) powder used in agar dilution and direct contact assays; and b) pressed disks used in biofilm-forming capability assay.

2.2. Characterization of materials

After the thermal treatments required to produce the desired chemical reactions, all samples were manually desegregated in an agate mortar, and powders with particle sizes of 25–75 μm were selected. X-ray diffraction (XRD) was used to analyze these powders using a Rigaku Ultima IV X-ray diffractometer operating with CuKα radiation (λ = 0.15418 nm). The diffraction patterns were obtained for 2θ, ranging from 10 to 70° in a continuous scan mode at 0.5°/min. To assist in structural characterization, the powders were also analyzed by Fourier transform infrared (FTIR) spectroscopy using a Perkin Elmer Spectrum GX model spectrometer operating in reflectance mode, with a spectral resolution of 4 cm^{-1} from 1400 to 400 cm^{-1}. The specific surface areas of the samples were determined using a Micromeritics ASAP 2020 analyzer by measuring the nitrogen adsorption isotherms at 77 K for use in the Brunauer-Emmett-Teller (BET) equation [38].

2.3. Evaluating in vitro bioactivity with ICG-TC04 method

The *in vitro* bioactivity of the particulate samples was evaluated according to the new ICG-TC04 method [30], proposed in 2015 by the Technical Committee 4 (TC04) of the International Commission on Glass (ICG) to overcome the limitations of ISO/FDIS 23317 [39], which was designed for solids with regular geometric shapes (i.e. disks or tiles) and not for powders or porous materials. Different to ISO/FDIS 23317, which establishes a relationship between apparent surface area (S_a) of the sample and volume of solution (V_sV) used in the test according to $V_s = S_a/10$, in the ICG-TC04 method there is a standardization based on concentration (mg/mL), with the assay being conducted under agitation. The solution used in this test is known as simulated body fluid (SBF), and is acellular, protein-free, and has a pH adjusted at 7.40 [40].

For this assay, the SBF was prepared according to Kokubo's method [40]. The ceramic powders were immersed into this solution using a ratio of 1.5 mg/mL (in triplicate). Each sample was cleaned ultrasonically for 10 s in acetone prior to its immersion in polyethylene bottles containing SBF. During the test, the powders were in contact with the solution for 3, 6, 12, 24, 48, 72, 96, 120, 144, 168, 336, 504, and 672 h, and the systems were kept under constant agitation at 37 °C

Table 1
Nominal composition of evaluated materials.

Sample	Components (mol%)								
	SiO_2	CaO	Na_2O	P_2O_5	Ag_2O	MgO	SrO	ZnO	Ga_2O_3
Bioglass®	46.14	26.91	24.35	2.60	–	–	–	–	–
Biosilicate®	49.16	25.79	23.33	1.72	–	–	–	–	–
Bio-FP	49.14	25.80	23.34	1.72	–	–	–	–	–
Bio-FP(Ag0.5)	49.62	26.05	23.57	0.50	0.25	–	–	–	–
Bio-FP(Ag1)	49.50	25.99	23.51	0.50	0.50	–	–	–	–
Bio-FP(Ag3)	49.00	25.72	23.28	0.50	1.50	–	–	–	–
Bio-FP(Mg0.5)	49.50	25.99	23.51	0.50	–	0.50	–	–	–
Bio-FP(Mg1)	49.25	25.86	23.39	0.50	–	1.00	–	–	–
Bio-FP(Mg3)	48.25	25.33	22.92	0.50	–	3.00	–	–	–
Bio-FP(Sr0.5)	49.50	25.99	23.51	0.50	–	–	0.50	–	–
Bio-FP(Sr1)	49.25	25.86	23.39	0.50	–	–	1.00	–	–
Bio-FP(Sr3)	48.25	25.33	22.92	0.50	–	–	3.00	–	–
Bio-FP(Zn0.5)	49.50	25.99	23.51	0.50	–	–	–	0.50	–
Bio-FP(Zn1)	49.25	25.86	23.39	0.50	–	–	–	1.00	–
Bio-FP(Zn3)	48.25	25.33	22.92	0.50	–	–	–	3.00	–
Bio-FP(Ga0.5)	49.62	26.05	23.57	0.50	–	–	–	–	0.25
Bio-FP(Ga1)	49.50	25.99	23.51	0.50	–	–	–	–	0.5
Bio-FP(Ga3)	49.00	25.72	23.28	0.50	–	–	–	–	1.50

on a shaker table. At the end of each test, samples were removed from bottles by filtration (particle retention > 3 μm) and rinsed with acetone to eliminate the SBF and terminate any surface reaction. After drying, a set of samples was analyzed using XRD, and by scanning electron microscopy (SEM) using an FEI Inspect S50 microscope to check for superficial HCA layer formation. Finally, the filtered solution was collected to determine the variations in pH that occurred throughout the test due to partial dissolution of the powders. For accomplishment of these measures, a Mettler Toledo S20 SevenEasy™ pH-meter was used.

2.4. Evaluation of antibacterial activity

Initially, samples with particle sizes 25–75 μm were subjected to wet milling with propan-2-ol ($CH_3CHOHCH_3$) in a high-energy planetary mill Pulverisette 6 using a jar and agate balls. After grinding, powders with a granulometry of less than 5 μm were selected by filtration and oven dried for use in agar dilution and direct contact assays. For the biofilm-forming capability, powders were compressed into disks measuring 10 mm in diameter and 2.2 mm in height by uniaxial pressing at 65 MPa (see Fig. 1). Particle sizes < 5 μm were chosen because they are suitable for the treatment of dentin hypersensitivity [34,41], as well as to investigate the influence of particle size of Biosilicate® comparing the results with those of a previous study [42], performed with particle sizes < 20 μm. Prior to the assays, all samples (powders and compressed disks) were first sterilized at 200 °C for 2 h, with reinforced attention to the samples containing silver.

Standard strains from the American Type Culture Collection (ATCC) and clinical bacteria isolated from oral and endodontic diseases selected for the study were anaerobic: *Peptostreptococcus micros* (clinical isolate), *Actinomyces viscosus* (clinical isolate), *A. naseslundii* (ATCC 19039), *A. naseslundii* (clinical isolate), *Fusobacterium nucleatum* (ATCC 25586), *F. nucleatum* (clinical isolate), *Prevotella intermedia* (clinical isolate), *P. nigrescens* (ATCC 33563), *P. buccae* (clinical isolate), *Porphyromonas gingivalis* (ATCC 33277), *P. gingivalis* (clinical isolate) and *Bacteroides fragilis* (ATCC 25285); and aerobic/microaerophilic: *Streptococcus salivarius* (ATCC 25975), *S. salivarius* (clinical isolate), *S. sobrinus* (ATCC 33478), *S. mutans* (ATCC 25175), *S. sanguinis* (ATCC 10556), *S. sanguinis* (clinical isolate), *S. mitis* (ATCC 49456), *Enterococcus faecalis* (ATCC 4082), *E. faecalis* (clinical isolate), *Lactobacillus casei* (ATCC 11578) and *L. casei* (clinical isolate). The culture media used for the anaerobic bacteria were Schaedler broth (Difco) supplemented with 1 μg/mL menadione and 5 μg/mL hemina (Sigma-Aldrich), and Schaedler agar (Difco) containing the same supplements plus 5% defibrinated sheep blood. For the aerobic/microaerophilic bacteria, Brain Heart Infusion — BHI broth (Difco) and BHI agar (Difco) were used, with 5% defibrinated sheep blood also being added to the agar.

2.4.1. Agar dilution method

To determine the MICs, the agar dilution method [43] was used, with some adaptations. All samples were diluted in test tubes so that when 18 mL of agar Schaedler or BHI were added in 2 mL of culture medium with each sample, the final concentrations reached 24, 16, 8, 4, 2, 1, and 0.5 mg/mL. Subsequently, tubes were homogenized and poured into appropriately coded Petri dishes (15 mm × 90 mm). The Schaedler and BHI broths were used without any sample as a negative control, while chlorhexidine gluconate solution (Sigma-Aldrich) was used for the positive control. All plates were prepared only at the time of assay.

The bacteria were cultured on Schaedler and BHI agar incubated at 36 °C during 24 h for aerobic/microaerophilic and 72 h for anaerobic microorganisms. In the case of anaerobic bacteria, all assays were performed in a MiniMac anaerobic chamber (Don Whitley Scientific) at 10% H_2, 10% CO_2, and 80% N_2. After incubation, bacterial suspensions were prepared from the cultures of each bacterium in respective broths and standardized to a turbidity corresponding to 0.5 on the McFarland scale (1.5×10^8 CFU/mL) for the aerobic/microaerophilic and 1.0 (3.0×10^8 CFU/mL) for anaerobic bacteria. Standardized suspensions were placed into a Steers multi-applicator and the Petri dishes labeled based on the positive control and from highest to lowest dilutions (ending on the negative control), in triplicate. Once the inoculants were dry, plates containing bacteria were then incubated in the same conditions described previously according to the specificity of each group of bacteria, with MIC values being determined as the lowest concentration of material capable of inhibiting visible growth of bacterial colonies in the culture media. We performed a statistical analysis using the ANOVA method with two criteria (material and bacterium) and a significance of 95%.

2.4.2. Biofilm-forming capability

To evaluate biofilm-forming capability, the pressed powders were used as a substrate for biofilm formation and growth employing adaptations of the methods described in other studies involving *E. coli* and *P. aeruginosa* [44], and *S. mutans* biofilms [45]. Overnight cultures of a set of aerobic bacteria and three days for anaerobic bacteria were re-suspended in broth to 1.0×10^7 CFU/mL, with aliquots of 200 μL then

being inoculated in 12-well microplates containing the disk samples and 4.8 mL of fresh broth (in triplicate). After incubation, maintaining the conditions of each bacteria group described previously, the spent growth medium containing nonadherent bacteria was removed and replaced with 5 mL of fresh medium. The plates were then incubated for a further 48 h to obtain a mature biofilm and 3 mL of fresh broth were added to the system for subsequent dilutions, plating and incubating at 36 °C to count bacterial colonies.

As a negative control, alumina (Al_2O_3) powder with particle sizes < 5 μm was compressed into disks and used in the assay due to its inert character, while for the positive control compressed disks of Bioglass® were used.

2.4.3. Direct contact method

For the direct contact assay [8,42], after incubation of a set of bacterial cultures, they were centrifuged at 4000 rpm for 5 min and washed with 0.9% sodium chloride (0.9% NaCl) solution. In the sequence, a new volume of solution was added to the sediment to reach a turbidity corresponding to approximately 3.0×10^8 CFU/mL. From each suspension, 10 μL were seeded onto the surface of the solid culture media (Schaedler and BHI agar) and the system was incubated at 36 °C for 24 and 72 h, as required by each bacterial group, for subsequent counting of colony-forming units per milliliter (CFU/mL) in triplicate assays.

Testing the samples, 25 mg of each of them were placed in Eppendorf-type microtubes (tubes 1 and 2) with 30 μL of bacterial suspension (1.0×10^6 CFU/mL). Tubes were them homogenized on a shaker for 10 min, with 470 μL of 0.9% NaCl solution added in tube 1. After 1 min of stirring, aliquots of 20 μL were removed from this tube and seeded onto the surface of the solid culture media for incubation and further reading of the bacterial growth — aliquots of 50 μL, obtained from serial dilutions ($0.1–1.0 \times 10^{-7}$) in NaCl solution, were similarly treated. Tube 2 remained incubated for 50 min and the same procedure described for tube 1 was used to evaluate possible viable cells. Thus, the samples remained in contact with the bacteria for a total period of 10 and 60 min. To verify the influence of pH, its value was measured for each testing time reproducing the same condition of the assay.

For this method, alumina was used as a negative control and Bioglass® as a positive control, both having the same granulometry (< 5 μm) as the other samples used in this assay.

3. Results and discussion

3.1. Characterization of materials

Fig. 2 shows the X-ray diffractogram of the sample Bio-FP and the others doped with 3 mol% Ag, Mg, Sr, Zn and Ga. The formation of sodium calcium silicate $Na_2CaSi_2O_6$ (PDF #77-2189) almost exclusively occurred from the proposed thermal treatment for all samples. The characteristic peak of another crystal phase, $Na_2Ca_2Si_3O_9$, also appears at ~25.89° (2θ), a result which is not surprising because it forms a solid solution with $Na_2CaSi_2O_6$ [46,47].

No other phases were identified with the incorporation of Ag, Mg, Sr, Zn, and Ga, therefore these elements remained in solid solution in the system. There was a mild displacement of some peaks, an observation which may be correlated to changes in lattice parameters, such as expansion or contraction of the unit cell of the major $Na_2CaSi_2O_6$ crystalline phase. Although the dopants Ag^{1+}, Mg^{2+}, Sr^{2+}, and Zn^{2+}, except Ga^{3+}, have similar oxidation numbers to Na^+ and Ca^{2+}, and were incorporated in small quantities, they have different ionic radii and electronegativity [48], explaining the small shifts in the diffraction pattern. Phosphorus (P^{5+}) also appears to have remained in solid solution because no other phase containing this element was identified. In relation to the strontium-containing samples, the precursor $SrCO_3$ was submitted to a previous treatment prior to incorporation into the system due to its high temperature for thermal decomposition (~1100 °C) [48] and formation of strontium oxide (SrO).

An important point is the formation of metallic silver (Ag^0) in the set of samples Bio-FP(Ag), evidenced by their slightly darkened color. In the standard silver diffraction sheet (PDF # 4-783), the most intense peak at ~38.17° (2θ) is very close to a peak of the $Na_2CaSi_2O_6$ phase. Within the resolution of the diffractograms, it was not possible to distinguish the contribution (intensity) of each of them. The concentration of silver is small. Furthermore, a certain silver fraction was segregated in the samples which could be removed using fine-tip tweezers. In any case, formation of Ag^0 was expected, as shown graphically in Fig. 3 by the change in the free energy of formation ($\Delta_f G^o$) of Ag_2O. During the synthesis procedure, silver is formed from the melting of the Ag_2SO_4 at ~660 °C [48]. At this temperature, Ag_2O is unstable due to the fact that above ~195 °C it is possible to observe positive values for $\Delta_f G^o$ [49,50]. This thermodynamic data indicates that silver remains reduced as Ag^0 above ~195 °C, with a fraction converted to Ag_2O just below this temperature in the cooling stage. To minimize this effect of silver reduction, all samples were synthesized under an O_2 atmosphere, shifting the equilibrium to the formation of Ag_2O.

The FTIR spectra of the doped samples (with 0.5 and 3 mol%) in Fig. 4 also did not show significant changes in relation to the undoped Bio-FP. All of them could be characterized by the presence of intense bands in the region of 1100 and 500 cm^{-1}. The bands at 1140, 1105 and 1040 cm^{-1} are related to the stretching vibrations of Si−O bonds [31,51,52]. For the samples doped with 3 mol%, comparing with the Bio-FP, discrete deformation can be observed in the band at ~940 cm^{-1}, which is attributed to the stretching vibrations of the non-bridging oxygen (NBO) bonds [31,51], formed by the presence of Na and Ca atoms. Such modification in this band is possibly related to the new modifying atoms (of the dopants) incorporated in the system. Another small modification is observed in the spectra of the samples containing Ag, the band situated at ~1105 cm^{-1} being more intense. This change occurred due to the presence of Ag, and not intensifying with an increase from 0.5 to 3 mol%, potentially being related to their segregation during the synthesis procedure.

Other intense vibrational bands characteristic of silicate compounds are observable at around 620 cm^{-1} for Si−O bond stretching, and at 535 and 465 cm^{-1} for Si−O bond bending [31,51,52]. Bands related to phosphorus were not observed, a result which can be explained by the low amount of P_2O_5 (1.72 mol%) in the system. Furthermore, the intense bands assigned to silicate groups overlap with some phosphate bands at around 1200 and 800 cm^{-1} for P−O bond stretching, and about 650 to 400 cm^{-1} for O−P−O bond bending related to the phosphate ions (PO_4^{3-}) vibrations [53].

The BET surface area found for Bioglass®, Biosilicate®, and Bio-FP were 0.71, 0.79, and 0.63 m^2/g, respectively, which are values typical for materials synthetized at high temperature. The doped samples were not analyzed, but similar values are expected because the thermal treatment applied for their synthesis was the same as that used for Bio-FP (1000 °C/480 min).

3.2. Evaluating in vitro bioactivity with ICG-TC04 method

By conducting the *in vitro* bioactivity test, we observed the formation of an HCA layer on sample surfaces from the time of 24 h. In the X-ray diffractograms of the Bioglass®, shown in Fig. 5, prior to the test (0 h) their glassy nature was confirmed by a broad halo centered at approximately 32° (2θ), which is typical of silicate glasses. After 12, 24, and 672 h of immersion in SBF, the formation of HCA is evident from 24 h by the presence of two intense peaks, near 26 and 32° (2θ), corresponding to (002) and (121) atomic plane diffractions of the HCA-like phase $Ca_5(PO_4)_3OH$ (PDF #84-1998). This association with HCA is made because the formation of pure hydroxyapatite on the glass surface is less likely to occur in SBF. This solution contains bicarbonate ions

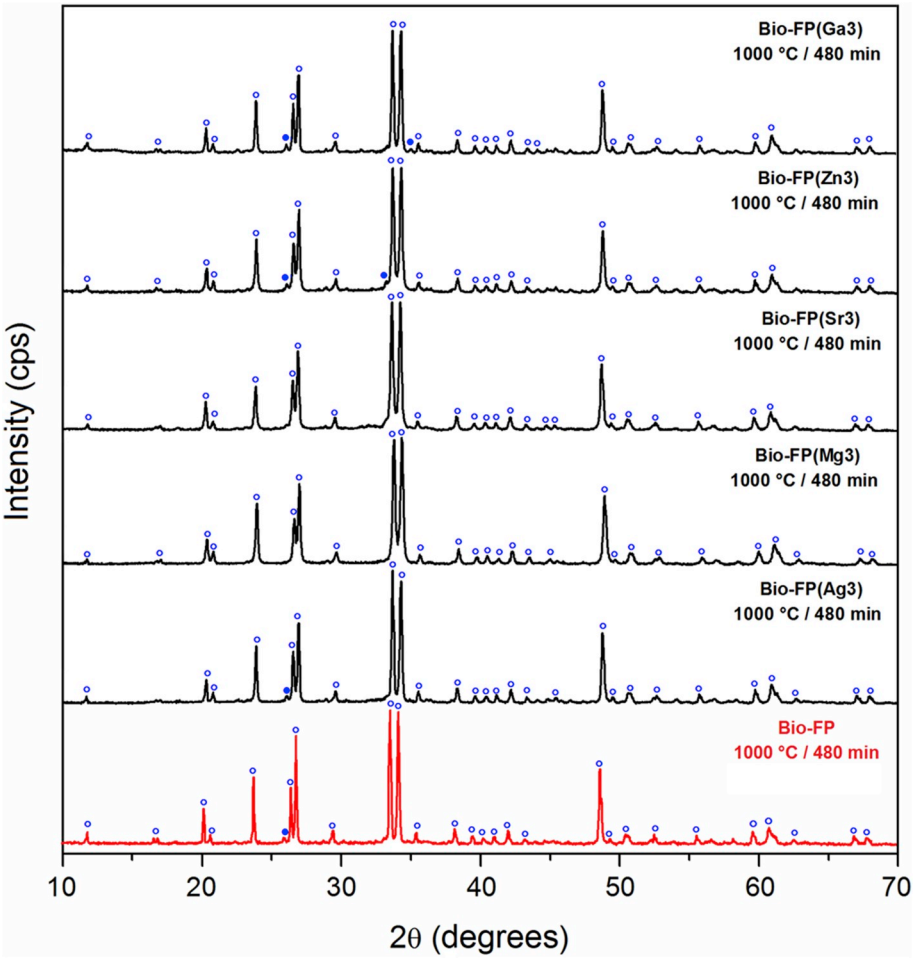

Fig. 2. XRD patterns of Bio-FP, Bio-FP(Ag3), Bio-FP(Mg3), Bio-FP(Sr3), Bio-FP(Zn3), and Bio-FP(Ga3): ○ = $Na_2CaSi_2O_6$ (PDF #77-2189); and ● = $Na_2Ca_2Si_3O_9$ (PDF #22-1455).

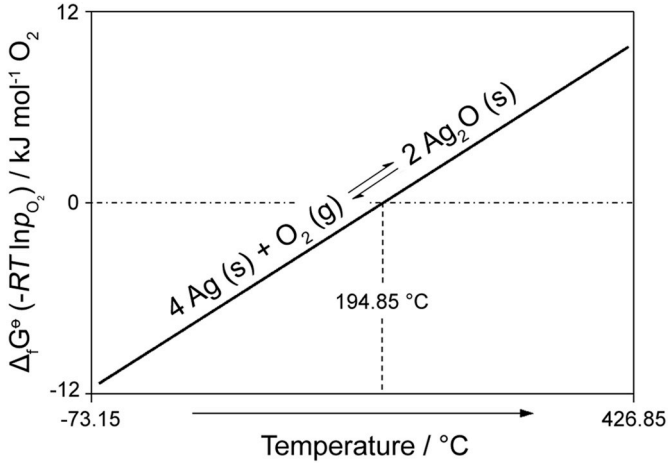

Fig. 3. Variation of free energy ($\Delta_f G^o$) as a function of temperature for formation of Ag_2O.

(HCO_3^-) and the hydroxyapatite is saturated with respect to slightly carbonated apatite, where orthophosphates are generally replaced by carbonates in the crystal lattice [30,54]. These main peaks increased with increasing testing time, and new peaks of low intensity appeared at approximately 40, 44, 50, 53, and 64° (2θ), corresponding, respectively, to the (310), (113), (123), (004), and (233) atomic planes in the hydroxyapatite lattice, which correlate with the increase in crystallinity.

The time of 24 h for the formation of HCA on the surface of the Bioglass® particles was the same as that reported by Maçon and co-authors [30]. Even the granulometry (25–75 *versus* 45–90 μm) and specific surface area (0.71 *versus* 0.24 m^2/g) of the material used here having a small variation compared to those of the aforementioned authors did not significantly affect *in vitro* bioactivity. For the Bioglass®, checking for HCA formation was easy and fast using XRD because it is a glassy material and the diffracted peaks that arise can be easily localized and characterized. In addition, the superficial change of the samples can also be accompanied by the presence of a new halo at ~22.50° (2θ), correlated to the formation of amorphous silica [1–3,37,51], which also increased in intensity as a function of the testing time.

For the crystalline samples (Biosilicate® and Bio-FP), the identification of the HCA layer formation required a more careful analysis. Biosilicate® and Bio-FP are constituted mostly by the $Na_2CaSi_2O_6$ crystal phase, and their diffraction pattern shows intense peaks in the same region (~25 and 34° (2θ)) as those of the HCA. Thus, although it was possible to identify the broad peaks at ~26 and 32° (2θ), both of which indicate the formation of HCA in the diffractograms of these samples from 24 h, as shown in Fig. 6, their intensities were low. Even with the testing time of 672 h, these peaks did not stand out in the diffractograms, showing only a small increase in intensity. Despite this problem, the superficial change of the samples can also be accompanied by the formation of a halo centered at ~22° (2θ), and by the decrease in intensity of some intrinsic peaks of the $Na_2CaSi_2O_6$ phase. Therefore, the ICG-TC04 method is also effective for evaluating the *in vitro* bioactivity of crystalline materials. However, for crystalline samples, particularly those with intense diffracted peaks at around 26 and 32° (2θ), the test needs to be performed carefully so that there is no misunderstanding

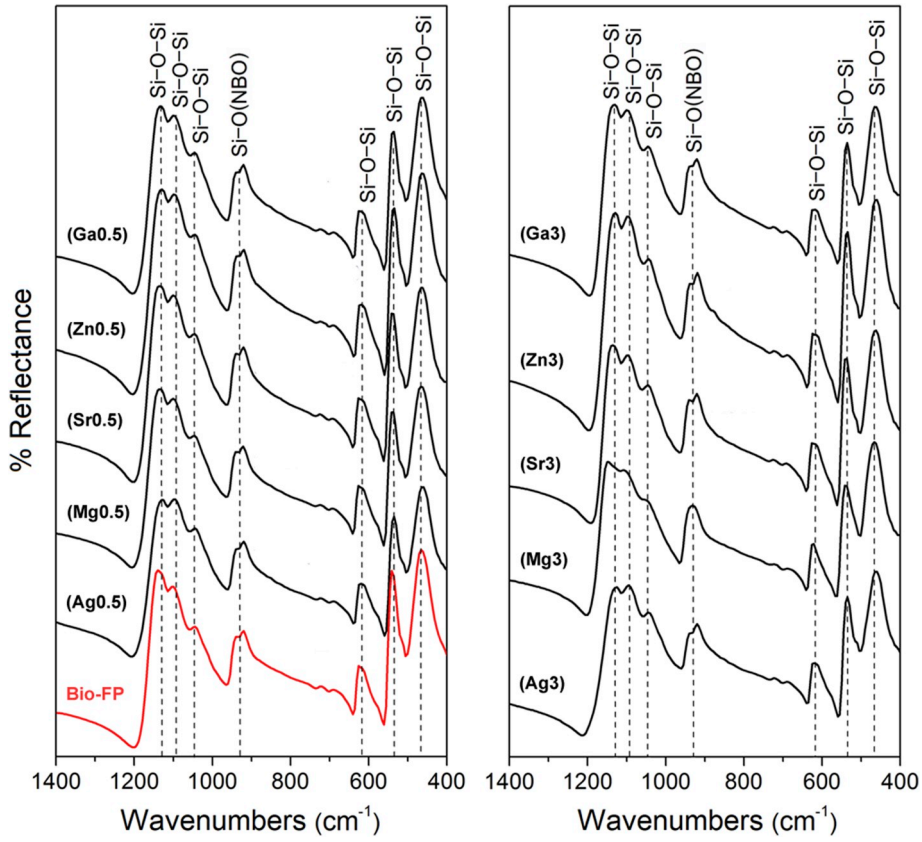

Fig. 4. FTIR spectra of Bio-FP, and Bio-FP(Ag), Bio-FP(Mg), Bio-FP(Sr), Bio-FP(Zn), and Bio-FP(Ga) doped with 0.5 and 3 mol%.

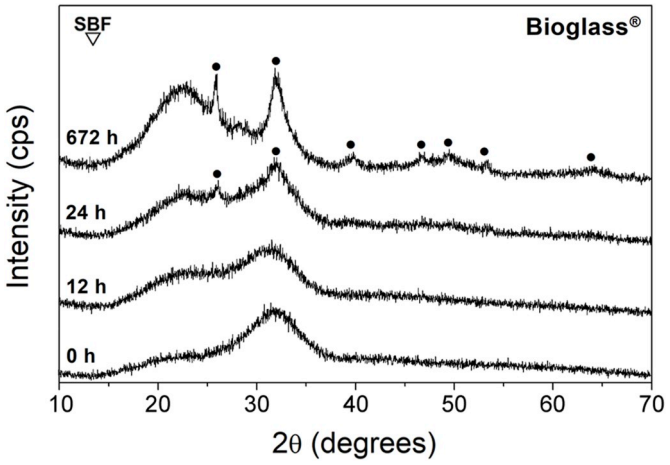

Fig. 5. XRD patterns of Bioglass® before and after immersion in SBF for 12, 24, and 672 h: ✱ = $Ca_5(PO_4)_3OH$ (PDF #84-1998).

because the results will not be as evident as in the case of glassy samples.

As shown by the SEM micrographs in Fig. 7, the morphology of the sample surfaces presented a certain change after various immersion times in SBF, resulting in a mixed polycrystalline thin layer of HCA. Prior to the test, the morphology of the particles was regular and smooth. After a test with duration of 24 h, the formation of a thin rough layer was noted. This layer grew as a function of time, but until 672 h it did not cover the entire surface of the particles homogeneously, a result which helps to explain, along with its small thickness, the high signal generated by the unreacted region (below this layer) of the samples, as observed in the X-ray diffractograms demonstrated in Figs. 5 and 6 (especially for crystalline ones).

Samples containing 0.5 mol% Ag, Mg, Sr, Zn, and Ga also exhibited HCA formation with 24 h immersion in SBF (diffractograms not shown). For the samples containing 1 and 3 mol%, the HCA formation was verified only after 120 h, as demonstrated in Fig. 8 for those doped with higher concentrations. The *in vitro* bioactivity of these samples decreased, and this effect was also observed with the modification of some glass compositions seeking for new properties and specific therapeutic activity [5,6]. For example, in a round robin study to validate the new ICG-TC04 method [30], a tested sample with similar composition to that of Bioglass® containing 2.4 mol% SrO exhibited the HCA formation from the testing time of 72 h in six of eight different laboratories where the tests were performed.

Beyond the characteristic peaks of the HCA that appear at ~26 and 32° (2θ), and the halo at ~22° (2θ), relative to the presence of amorphous silica, in the set of samples Bio-FP(Ag) immersed in SBF it was also possible to identify the formation of silver chloride (AgCl). A sharp peak appeared at ~32.24° (2θ) after the first testing time of 3 h. This peak surpassed that of the HCA located in the same region, as can be observed in Fig. 8. Other low intensity peaks at approximately 27.82, 46.22, 54.86, and 57.54° (2θ) were also noted in the diffractogram confirming the AgCl formation, which could be monitored indirectly by the color change of the samples during each testing time. In the SBF solution, chloride ions (Cl^-) are present [40], which react with Ag^+ released from the sample forming a precipitate of AgCl due to their solubility product constant being low ($Kps_{AgCl} = 1.77 \times 10^{-10}$) — exhibiting a solubility in aqueous medium of approximately 1.9×10^{-3} g/L [48]. The presence of silver chloride did not inhibit HCA formation, but we did not find in the literature its influence on the biological properties of similar bioactive materials, an area which needs to be further investigated.

Fig. 9 illustrates the variations in pH as a function of the immersion time of samples in SBF. With the exception of the Bioglass®, which presented the largest global variation, reaching a mean value of 8.7 in

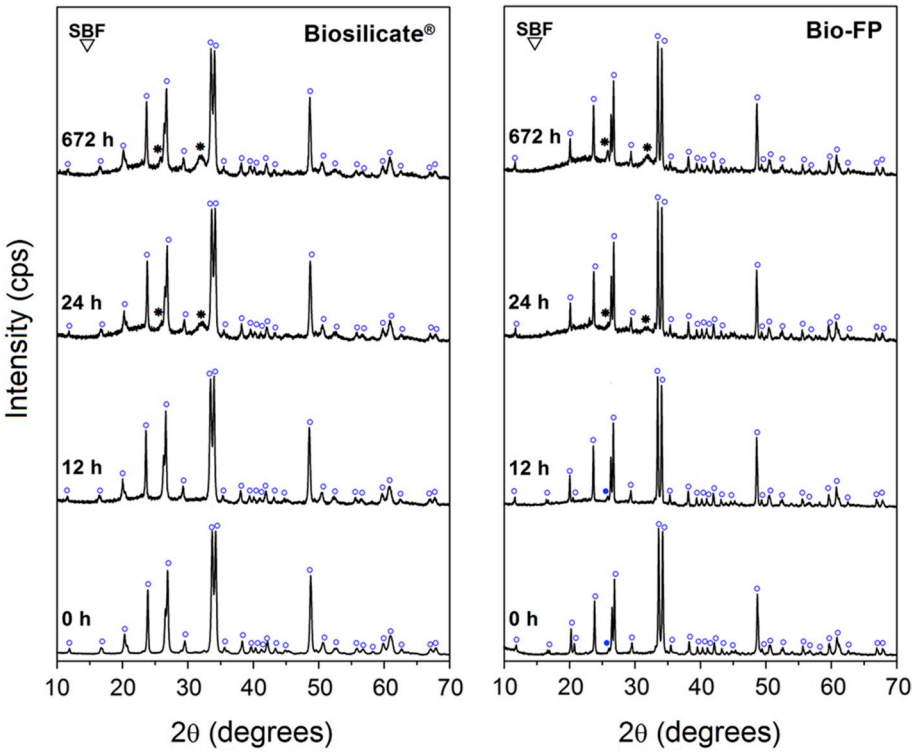

Fig. 6. XRD patterns of Biosilicate® and Bio-FP before and after immersion in SBF for 12, 24, and 672 h: ○ = $Na_2CaSi_2O_6$ (PDF #77-2189); ● = $Na_2Ca_2Si_3O_9$ (PDF #22-1455); and ✱ = $Ca_5(PO_4)_3OH$ (PDF #84-1998).

the last testing time (672 h), the other samples demonstrated very similar behavior. They provided a rapid variation in the first hours, reaching a pH of ~8.2 and remained around this value until the last test. Hence, the incorporation of Ag, Mg, Sr, Zn, and Ga in some crystalline samples, with a concentration range of 0.5–3 mol%, did not cause a significant reduction in their solubility because the pH variation has a relationship with this property [1–3,30,31,37,51]. Bioglass®, for example, is a glassy material and tends to have a higher solubility than

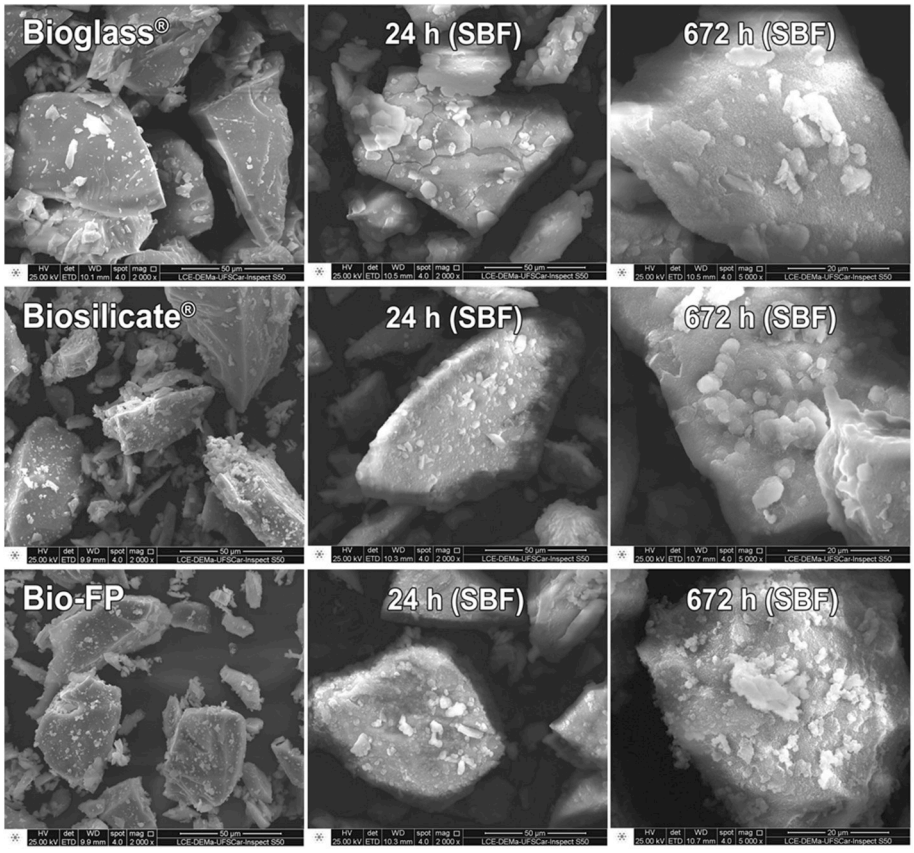

Fig. 7. SEM micrographs of Bioglass®, Biosilicate®, and Bio-FP before and after immersion in SBF for 24 and 672 h.

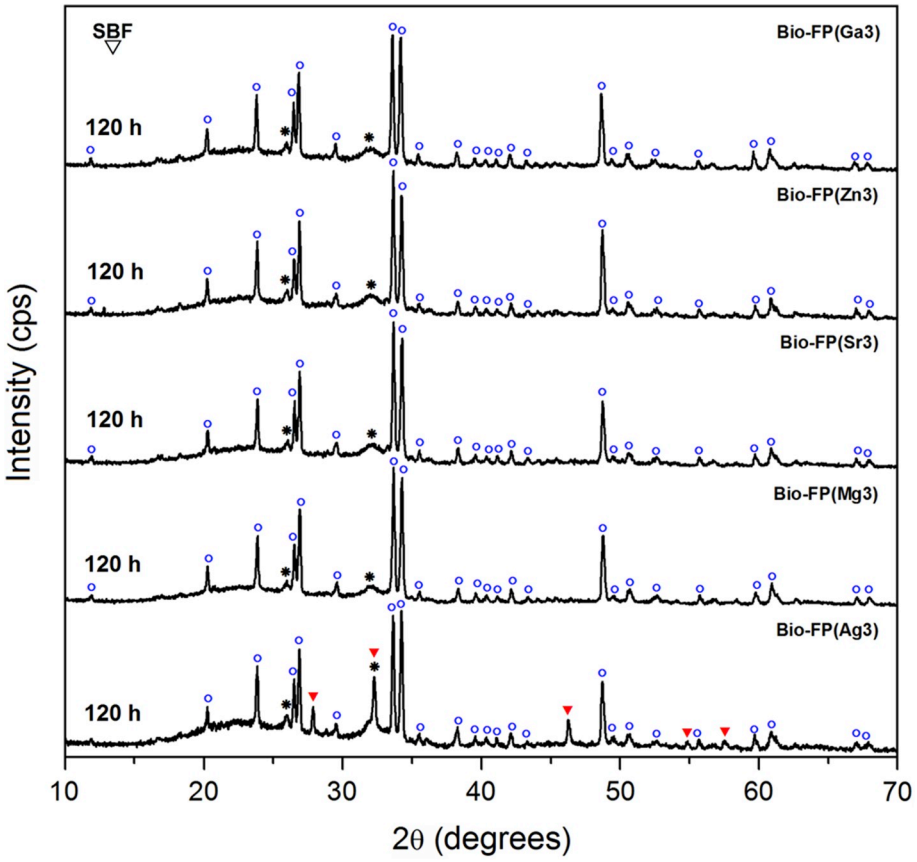

Fig. 8. XRD patterns of Bio-FP(Ag3), Bio-FP(Mg3), Bio-FP(Sr3), Bio-FP(Zn3), and Bio-FP(Ga3) after immersion in SBF for 120 h: ○ = $Na_2CaSi_2O_6$ (PDF #77-2189); ✱ = $Ca_5(PO_4)_3OH$ (PDF #84-1998); and ▼ = AgCl (PDF #31-1238).

its crystalline counterparts (considering similar compositions). This phenomenon could be observed by the higher pH variation that it promoted in the test, due to the number of cations (Na^+ and Ca^{2+}) exchanged from the sample with H^+ to the SBF solution. These results show a correlation with observations verified in the antibacterial activity assays, as discussed below, in which only the intrinsic effect of some incorporated elements, particularly silver, was found. The increase in their concentrations did not intensify the antibacterial effect against the tested microorganisms.

3.3. Evaluation of antibacterial activity

3.3.1. Agar dilution method

Bioglass®, Biosilicate®, and Bio-FP showed inhibitory activity for most of the bacteria evaluated in the concentration range of 0.5–24 mg/mL, as shown in Table 2. MIC values found for the samples containing Ag, Mg, Sr, Zn, and Ga are shown in Tables 3 and 4. The low values of MIC found for the chlorhexidine gluconate solution compared to the samples were expected because it is a well-known disinfectant and was used as a positive control of the method to confirm bacterial death.

In general, the MIC values found for Bioglass® were similar to those determined for Biosilicate® and Bio-FP. From the total of 23 bacteria evaluated, the anaerobic *P. micros* (clinical isolate), *A. viscosus* (clinical isolate), *A. naeslundii* (clinical isolate), *P. intermedia* (clinical isolate), *B. fragilis* (ATCC 25285), *P. nigrescens* (ATCC 33563), *P. buccae* (clinical isolate), and the aerobic *E. faecalis* (ATCC 4082/clinical isolate) were not sensitive to the materials in the range of 0.5–24 mg/mL. The highest concentration (24 mg/mL) of the samples established for the assays was not sufficient to promote an effect in these bacteria, although this result does not mean that such an effect would not be observed at higher concentrations. Although the samples containing Ag, Mg, Sr, Zn, and Ga have shown an effect against *P. nigrescens* (ATCC 33563), the inhibitory effect against all other bacteria was only observed with the samples containing silver in their composition, as can be seen in Tables 3 and 4. Hence, the intrinsic effect of Ag is apparent, with this element already being well known for its broad spectrum antimicrobial activity [16,17].

Assessing the antibacterial activity of 0.05, 0.1, and 0.2 μg/mL silver ion solutions, Jung and coauthors [55] demonstrated the better efficacy of these solutions against Gram-negative *E. coli* compared to Gram-positive *S. aureus*. According to these authors, this observation was possibly due to differences in the cell wall of each type of bacteria — Gram-positive bacteria have a thick layer of peptidoglycan, which may prevent the action of the silver ions through the bacterial cell wall in relation to the Gram-negative bacteria. Checking this hypothesis by transmission electron microscopy, they demonstrated considerable changes in bacterial cell membranes upon silver ion treatment which have been the cause or consequence of cell death, besides helping to explain the different cellular responses for both Gram-positive and -negative bacteria. Undoubtedly, these data are very interesting and enrich the discussion because our results in Table 3 for the samples containing silver followed the same trend. In general, with the lowest MIC values were achieved for Gram-negative *F. nucleatum*, *P. intermedia*, *P. gingivalis*, *B. fragilis*, *P. nigrescens*, and *P. buccae* when compared with the Gram-positive bacteria evaluated.

Analyzing other doped samples, even those containing 6 mol% of Ga and Zn (data not shown), elements with recognized activity against certain microorganisms when incorporated in similar materials [24,56–58], demonstrated no effect. Clearly, such comparisons are only qualitative because this property depends on the degradation rate of the material, the concentration of the dopant, and also the type of microorganism evaluated. For example, when boron (B) is employed for the formulation of borate glasses (high concentrations), it contributes to antimicrobial activity [59], in addition to being considered a potential stimulating agent in the process of bone regeneration [5,60]. On the other hand, the incorporation of small amounts (2 wt%) of B_2O_3 into Bioglass® does not seem to promote an effect, at least against *S. aureus*

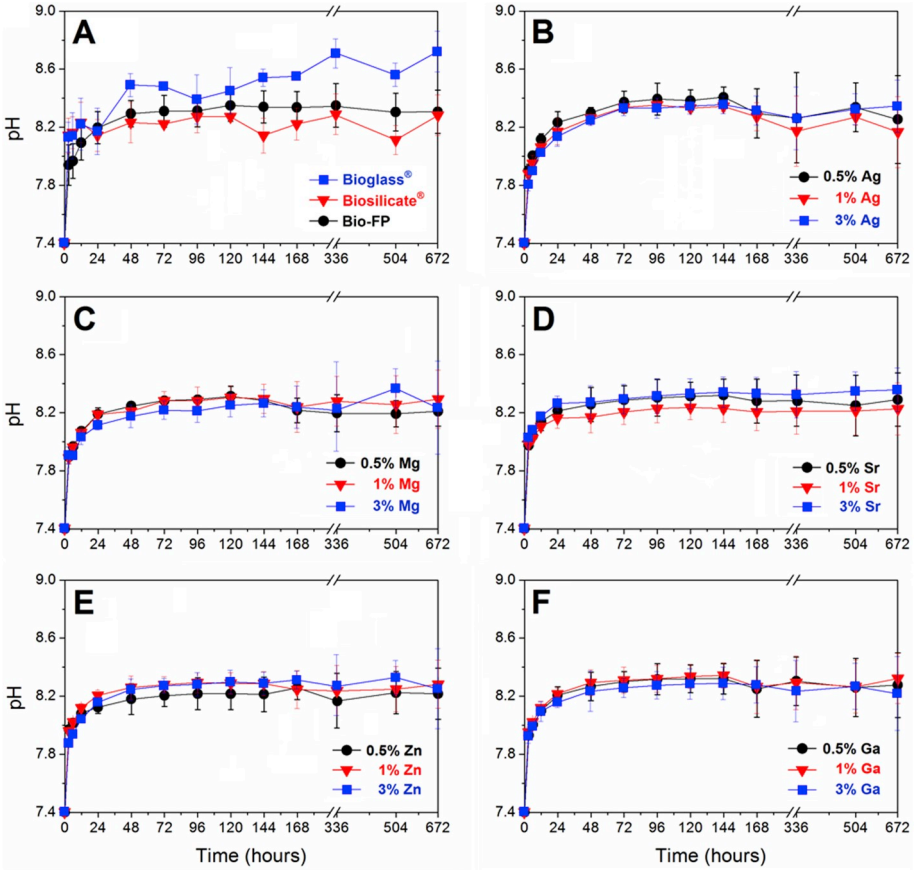

Fig. 9. Variations in pH as a function of immersion time of samples in SBF: A) Bioglass®, Biosilicate® and Bio-FP; B) set of samples Bio-FP(Ag); C) set of samples Bio-FP (Mg); D) set of samples Bio-FP(Sr); E) set of samples Bio-FP(Zn); and F) set of samples Bio-FP(Ga).

[61].

For the set of samples Bio-FP(Ag), increasing the silver content from 0.5 to 3 mol% provided an improvement in the results, decreasing the MIC values required for the inhibition of most bacteria. This tendency was also observed only for the samples Bio-FP(Sr) against *S. salivarius* (ATCC 33478/clinical isolate) and *S. sanguinis* (ATCC 10556), as shown in Tables 3 and 4. Another factor (together with dopant concentration) that did not influence the antibacterial activity of the materials was particle size variation. In this study, we used powders with particle sizes of less than 5 μm, except for the set of samples Bio-FP(Ag), which were reactive during wet milling. The propan-2-ol oxidized while the silver ions reduced, causing the formation of a dark brown pasty mixture. Consequently, we used powders with a granulometry of less than 25 μm, obtained by manual grinding in an agate mortar. Moreover, a sample of Bioglass® (data not shown) with the same granulometry (< 25 μm) was tested, and there was no statistical difference in the results compared with the samples with particle sizes < 5 μm.

Comparing our results with those reported by Martins and colleagues [42], we also did not find a significant difference in relation to the particle sizes. In that study, the authors evaluated the antimicrobial activity of Biosilicate® using the same method (agar dilution) but starting from a sample with particle sizes of 0.1–20 μm. Although this variation in granulometry on the microscale did not influence the antibacterial activity of the material, a reduction to nanoscale, on the other hand, makes a noticeable difference. The antibacterial properties of interest observed for Bioglass®, in the case of commercially available versions such as PerioGlas, are usually attributed to the continuous release of alkaline species in the medium where it is inserted. Testing the hypothesis that, with a larger surface area, a nanometric glass releases more alkaline species and, consequently, has a more pronounced antibacterial effect, Waltimo and coauthors [62] synthesized powders with particle sizes of approximately 30 nm and composition close to that of Bioglass®. When immersed in a phosphate-buffered saline solution (PBS), this sample promoted a 10-fold increase in the silica release and the pH reached values close to 12 *versus* 8 when compared with the PerioGlas with particle sizes of ~100 μm. The higher solubility of this nanometric glass provided a substantial increase in antibacterial activity against *E. faecalis* (ATCC 29212/clinical isolate), which, as we have seen in the present study, are quite resistant to the presence of similar materials of the $SiO_2-CaO-Na_2O-P_2O_5$ system.

Therefore, an explanation for not observing a difference in the results of MIC comparing the materials evaluated is that they have very close degradation rates in an aqueous medium. This suggestion could be verified indirectly by the result shown in Fig. 9 regarding the pH variation monitored in SBF during the *in vitro* bioactivity test. The pH reached values of approximately 8.2 after a rapid variation in the first hours and was practically constant until the end of the test, with a duration of 672 h. These data indicate that the samples exhibited some degree of antibacterial effect with consequent elevation of pH of the medium, leading to a rapid change in local osmotic pressure, causing cellular injury. In addition, although it was not possible to verify a considerable influence of the variation in Mg, Sr, Zn, and Ga concentration in the samples, their presence also contributed to promoting an inhibitory effect. The highlight is the samples containing Ag, due to their higher broad spectrum of action achieved with the incorporation of this element. It is important to note that the minimum bactericidal concentration reported for silver ions is approximately 0.1 mg/L and their cytotoxic levels for human cells are > 1.6 mg/L [63]. Thus, the set of samples Bio-FP(Ag) and those doped with different elements should be studied regarding their ion release profile and cytotoxicity, so that new applications can be successfully designed.

Finally, it should be mentioned that the antibacterial effect of the

Table 2
MIC (mg/mL) values for Bioglass®, Biosilicate®, and Bio-FP. Positive control: chlorhexidine gluconate.

Bacteria	Positive control	Bioglass®	Biosilicato®	Bio-FP
P. micros (clinical isolate)	$0.128_{A,a}$	$> 24_{A,b}$	$> 24_{A,b}$	$> 24_{A,b}$
A. viscosus (clinical isolate)	$0.064_{B,a}$	$> 24_{A,b}$	$> 24_{A,b}$	$> 24_{A,b}$
A. naeslundii (ATCC 19039)	$0.016_{C,a}$	$4_{B,b}$	$4_{B,b}$	$8_{B,c}$
A. naeslundii (clinical isolate)	$0.008_{C,a}$	$> 24_{A,b}$	$> 24_{A,b}$	$> 24_{A,b}$
F. nucleatum (ATCC 25586)	$0.032_{C,a}$	$16_{C,b}$	$16_{C,b}$	$4_{C,c}$
F. nucleatum (clinical isolate)	$0.001_{C,a}$	$16_{C,b}$	$16_{C,b}$	$4_{C,c}$
P. intermedia (clinical isolate)	$0.016_{C,a}$	$> 24_{A,b}$	$> 24_{A,b}$	$> 24_{A,b}$
P. gingivalis (ATCC 33277)	$0.016_{C,a}$	$4_{B,b}$	$4_{B,b}$	$4_{C,b}$
P. gingivalis (clinical isolate)	$0.001_{C,a}$	$8_{D,b}$	$8_{D,b}$	$4_{C,c}$
B. fragilis (ATCC 25285)	$2.04_{D,a}$	$> 24_{A,b}$	$> 24_{A,b}$	$> 24_{A,b}$
P. nigrescens (ATCC 33563)	$0.016_{C,a}$	$> 24_{A,b}$	$> 24_{A,b}$	$> 24_{A,b}$
P. buccae (clinical isolate)	$0.032_{C,a}$	$> 24_{A,b}$	$> 24_{A,b}$	$> 24_{A,b}$
S. salivarius (ATCC 25975)	$0.002_{A,a}$	$2_{A,b}$	$2_{A,b}$	$8_{A,c}$
S. salivarius (clinical isolate)	$0.002_{A,a}$	$2_{A,b}$	$2_{A,b}$	$8_{A,c}$
E. faecalis (ATCC 4082)	$0.008_{A,a}$	$> 24_{B,b}$	$> 24_{B,b}$	$> 24_{B,b}$
E. faecalis (clinical isolate)	$0.008_{A,a}$	$> 24_{B,b}$	$> 24_{B,b}$	$> 24_{B,b}$
S. sobrinus (ATCC 33478)	$0.001_{A,a}$	$4_{C,b}$	$8_{C,c}$	$2_{C,d}$
S. mutans (ATCC 25175)	$0.001_{A,a}$	$4_{C,b}$	$4_{D,b}$	$2_{C,c}$
S. sanguinis (ATCC 10556)	$0.002_{A,a}$	$8_{D,b}$	$8_{C,b}$	$8_{A,b}$
S. sanguinis (clinical isolate)	$0.004_{A,a}$	$16_{E,b}$	$0.5_{E,c}$	$16_{E,b}$
S. mitis (ATCC 49456)	$0.002_{A,a}$	$8_{D,b}$	$2_{A,c}$	$2_{C,c}$
L. casei (ATCC 11578)	$0.002_{A,a}$	$4_{C,b}$	$4_{D,b}$	$1_{D,c}$
L. casei (clinical isolate)	$0.002_{A,a}$	$4_{C,b}$	$4_{D,b}$	$1_{D,c}$

*Different letters indicate statistical difference (significance equal to 95%).

samples against standard strains and the clinical isolates, in general, were similar, having only a higher sensitivity of the *S. sanguinis* clinical isolate when compared with the standard strain (ATCC 10556). These results indicate that both standard strains, as well as the clinical isolates, showed practically the same behavior in the presence of the different samples evaluated, which enables these materials to be tested in procedures of prophylaxis and treatments of oral infections. It is worth emphasizing that all of these materials presented a broad spectrum of antibacterial activity even in a low concentration range (0.5–24 mg/mL), which is much lower than those normally used in dental applications.

3.3.2. Biofilm-forming capability

Table 5 illustrates the result of the biofilm-forming capability assay for Bioglass®, Biosilicate®, and Bio-FP, in which it is possible to observe the inhibition of bacterial biofilm formation for all microorganisms. Because the undoped sample Bio-FP already exhibited a bactericidal effect similar to Bioglass® and Biosilicate®, used as a reference, we did not analyze the samples containing Ag, Mg, Sr, Zn, and Ga. Evaluating alumina as a negative control, we can infer that it had no effect on inhibiting bacteria, and the results observed for the other samples are solely due to their nature. The alumina is a very stable material and did not exhibit any antibacterial activity. Consequently, the positive results are directly related to the different samples tested, without interference from the culture medium. An example of sample's stability that is not completely inert, consequently with low solubility and antibiofilm effect, is a gel-glass with 80 mol% SiO_2 [45]. This glass is bioactive and can promote stem cell proliferation, but its relative stability in an aqueous medium demonstrates that the *S. mutans* biofilm has the capacity to adhere to the glass surface, thus not promoting an unfavorable environment capable of inhibiting biofilm formation — at least for this bacterium.

Regarding the bacteria selected for this assay, most of them are commonly associated with failures in endodontic treatment and root canal infection [64–66]. In addition, a consequence of biofilm formation by oral bacteria is their ability to increase tolerance to antimicrobial agents, including those used in toothpastes, mouthwashes, and antibiotics, as well as the pathogenic synergism [67]. Therefore, the results of the antibiofilm effect shown in Table 5 are significant because they demonstrate that Bio-FP has a strong antibacterial property, similar to Bioglass® and Biosilicate®, being capable of inhibiting

Table 3
MIC (mg/mL) values for the set of samples Bio-FP(Ag) and Bio-FP(Mg).

Bacteria	Ag			Mg		
	0.5%	1%	3%	0.5%	1%	3%
P. micros (clinical isolate)	$24_{A,a}$	$24_{A,a}$	$16_{A,b}$	$> 24_{A,a}$	$> 24_{A,a}$	$> 24_{A,a}$
A. viscosus (clinical isolate)	$4_{B,a}$	$4_{B,a}$	$4_{B,a}$	$> 24_{A,a}$	$> 24_{A,a}$	$> 24_{A,a}$
A. naeslundii (ATCC 19039)	$2_{D,a}$	$2_{D,a}$	$1_{C,a}$	$8_{B,a}$	$8_{B,a}$	$8_{B,a}$
A. naeslundii (clinical isolate)	$8_{C,a}$	$8_{C,a}$	$4_{B,b}$	$> 24_{A,a}$	$> 24_{A,a}$	$> 24_{A,a}$
F. nucleatum (ATCC 25586)	$1_{D,a}$	$1_{D,a}$	$1_{C,a}$	$8_{B,a}$	$8_{B,a}$	$8_{B,a}$
F. nucleatum (clinical isolate)	$1_{D,a}$	$1_{D,a}$	$1_{C,a}$	$8_{B,a}$	$8_{B,a}$	$8_{B,a}$
P. intermedia (clinical isolate)	$4_{B,a}$	$4_{B,a}$	$2_{C,b}$	$> 24_{A,a}$	$> 24_{A,a}$	$> 24_{A,a}$
P. gingivalis (ATCC 33277)	$1_{D,a}$	$1_{D,a}$	$1_{C,a}$	$4_{C,a}$	$4_{C,a}$	$4_{C,a}$
P. gingivalis (clinical isolate)	$4_{C,a}$	$4_{C,a}$	$4_{C,a}$	$4_{C,a}$	$4_{C,a}$	$4_{C,a}$
B. fragilis (ATCC 25285)	$4_{A,a}$	$16_{E,b}$	$8_{D,c}$	$> 24_{A,a}$	$> 24_{A,a}$	$> 24_{A,a}$
P. nigrescens (ATCC 33563)	$8_{C,a}$	$8_{C,a}$	$8_{D,a}$	$4_{C,a}$	$4_{C,a}$	$4_{C,a}$
P. buccae (clinical isolate)	$8_{C,a}$	$8_{C,a}$	$8_{D,a}$	$> 24_{A,a}$	$> 24_{A,a}$	$> 24_{A,a}$
S. salivarius (ATCC 25975)	$16_{A,a}$	$16_{A,a}$	$8_{A,b}$	$8_{A,a}$	$8_{A,a}$	$8_{A,a}$
S. salivarius (clinical isolate)	$16_{A,a}$	$8_{B,b}$	$4_{B,c}$	$8_{A,a}$	$8_{A,a}$	$8_{A,a}$
E. faecalis (ATCC 4082)	$16_{A,a}$	$16_{A,a}$	$8_{A,b}$	$> 24_{B,a}$	$> 24_{B,a}$	$> 24_{B,a}$
E. faecalis (clinical isolate)	$16_{A,a}$	$16_{A,a}$	$8_{A,b}$	$> 24_{B,a}$	$> 24_{B,a}$	$> 24_{B,a}$
S. sobrinus (ATCC 33478)	$4_{B,a}$	$8_{B,b}$	$2_{C,c}$	$2_{C,a}$	$2_{C,a}$	$2_{C,a}$
S. mutans (ATCC 25175)	$8_{C,a}$	$8_{B,a}$	$2_{C,b}$	$2_{C,a}$	$2_{C,a}$	$2_{C,a}$
S. sanguinis (ATCC 10556)	$16_{A,a}$	$8_{B,b}$	$4_{B,c}$	$8_{A,a}$	$8_{A,a}$	$8_{A,a}$
S. sanguinis (clinical isolate)	$1_{D,a}$	$1_{C,a}$	$1_{C,a}$	$2_{C,a}$	$2_{C,a}$	$2_{C,a}$
S. mitis (ATCC 49456)	$2_{D,a}$	$2_{C,a}$	$2_{C,a}$	$1_{D,a}$	$1_{D,a}$	$1_{D,a}$
L. casei (ATCC 11578)	$4_{B,a}$	$4_{D,a}$	$4_{B,a}$	$4_{E,a}$	$4_{E,a}$	$4_{E,a}$
L. casei (clinical isolate)	$4_{B,a}$	$4_{D,a}$	$1_{C,b}$	$2_{C,a}$	$2_{C,a}$	$2_{C,a}$

*Different letters indicate statistical difference (significance equal to 95%).

Table 4
MIC (mg/mL) values for the set of samples Bio-FP(Sr), Bio-FP(Zn), and Bio-FP(Ga).

Bacteria	Sr			Zn				Ga	
	0.5%	1%	3%	0.5%	1%	0.5%	0.5%	0.5%	3%
P. micros (clinical isolate)	$>24_{A,a}$	$>24_{A,a}$	$>24_{A,a}$	$>24_{A,a}$	$>24_{A,a}$	$>24_{A,a}$	$>24_{A,a}$	$>24_{A,a}$	$>24_{A,a}$
A. viscosus (clinical isolate)	$>24_{A,a}$	$>24_{A,a}$	$>24_{A,a}$	$>24_{A,a}$	$>24_{A,a}$	$>24_{A,a}$	$>24_{A,a}$	$>24_{A,a}$	$>24_{A,a}$
A. naeslundii (ATCC 19039)	$8_{B,a}$	$8_{B,a}$	$8_{B,a}$	$8_{B,a}$	$8_{B,a}$	$16_{B,a}$	$16_{B,a}$	$16_{B,a}$	$16_{B,a}$
A. naeslundii (clinical isolate)	$>24_{A,a}$	$>24_{A,a}$	$>24_{A,a}$	$>24_{A,a}$	$>24_{A,a}$	$>24_{A,a}$	$>24_{A,a}$	$>24_{A,a}$	$>24_{A,a}$
F. nucleatum (ATCC 25586)	$4_{C,a}$	$4_{C,a}$	$4_{C,a}$	$8_{B,a}$	$8_{B,a}$	$8_{C,a}$	$8_{C,a}$	$8_{C,a}$	$8_{C,a}$
F. nucleatum (clinical isolate)	$8_{B,a}$	$8_{B,a}$	$8_{B,a}$	$8_{B,a}$	$8_{B,a}$	$16_{B,a}$	$16_{B,a}$	$16_{B,a}$	$16_{B,a}$
P. intermedia (clinical isolate)	$>24_{A,a}$	$>24_{A,a}$	$>24_{A,a}$	$>24_{A,a}$	$>24_{A,a}$	$>24_{A,a}$	$>24_{A,a}$	$>24_{A,a}$	$>24_{A,a}$
P. gingivalis (ATCC 33277)	$2_{D,a}$	$2_{D,a}$	$2_{D,a}$	$4_{C,a}$	$4_{C,a}$	$8_{C,a}$	$8_{C,a}$	$8_{C,a}$	$8_{C,a}$
P. gingivalis (clinical isolate)	$4_{C,a}$	$4_{C,a}$	$4_{C,a}$	$8_{B,a}$	$8_{B,a}$	$8_{C,a}$	$8_{C,a}$	$8_{C,a}$	$8_{C,a}$
B. fragilis (ATCC 25285)	$>24_{A,a}$	$>24_{A,a}$	$>24_{A,a}$	$>24_{A,a}$	$>24_{A,a}$	$>24_{A,a}$	$>24_{A,a}$	$>24_{A,a}$	$>24_{A,a}$
P. nigrescens (ATCC 33563)	$4_{C,a}$	$4_{C,a}$	$4_{C,a}$	$8_{B,a}$	$8_{B,a}$	$8_{C,a}$	$8_{C,a}$	$8_{C,a}$	$8_{C,a}$
P. buccae (clinical isolate)	$>24_{A,a}$	$>24_{A,a}$	$>24_{A,a}$	$>24_{A,a}$	$>24_{A,a}$	$>24_{A,a}$	$>24_{A,a}$	$>24_{A,a}$	$>24_{A,a}$
S. salivarius (ATCC 25975)	$16_{A,a}$	$8_{A,b}$	$8_{A,b}$	$8_{A,a}$	$8_{A,a}$	$16_{A,a}$	$16_{A,a}$	$16_{A,a}$	$16_{A,a}$
S. salivarius (clinical isolate)	$16_{A,a}$	$8_{A,b}$	$8_{A,b}$	$8_{A,a}$	$8_{A,a}$	$16_{A,a}$	$16_{A,a}$	$16_{A,a}$	$16_{A,a}$
E. faecalis (ATCC 4082)	$>24_{B,a}$	$>24_{B,a}$	$>24_{B,a}$	$>24_{B,a}$	$>24_{B,a}$	$>24_{B,a}$	$>24_{B,a}$	$>24_{B,a}$	$>24_{B,a}$
E. faecalis (clinical isolate)	$>24_{B,a}$	$>24_{B,a}$	$>24_{B,a}$	$>24_{B,a}$	$>24_{B,a}$	$>24_{B,a}$	$>24_{B,a}$	$>24_{B,a}$	$>24_{B,a}$
S. sobrinus (ATCC 33478)	$2_{C,a}$	$2_{C,a}$	$2_{C,a}$	$2_{C,a}$	$2_{C,a}$	$4_{C,a}$	$4_{C,a}$	$4_{C,a}$	$4_{C,a}$
S. mutans (ATCC 25175)	$2_{C,a}$	$2_{C,a}$	$2_{C,a}$	$2_{C,a}$	$2_{C,a}$	$2_{C,a}$	$2_{C,a}$	$2_{C,a}$	$2_{C,a}$
S. sanguinis (ATCC 10556)	$16_{A,a}$	$8_{A,b}$	$8_{A,b}$	$8_{A,a}$	$8_{A,a}$	$24_{D,a}$	$24_{D,a}$	$24_{D,a}$	$24_{D,b}$
S. sanguinis (clinical isolate)	$8_{E,a}$	$8_{E,a}$	$8_{E,a}$	$8_{A,a}$	$8_{A,a}$	$1_{E,a}$	$1_{E,a}$	$1_{E,a}$	$1_{D,a}$
S. mitis (ATCC 49456)	$2_{C,a}$	$2_{C,a}$	$2_{C,a}$	$2_{C,a}$	$2_{C,a}$	$2_{E,a}$	$2_{E,a}$	$2_{E,a}$	$2_{C,a}$
L. casei (ATCC 11578)	$4_{D,a}$	$4_{D,a}$	$4_{D,a}$	$4_{D,a}$	$4_{D,a}$	$4_{C,a}$	$4_{C,a}$	$4_{C,a}$	$4_{C,a}$
L. casei (clinical isolate)	$2_{C,a}$	$2_{C,a}$	$2_{C,a}$	$2_{C,a}$	$2_{C,a}$	$4_{C,a}$	$4_{C,a}$	$4_{C,a}$	$4_{C,a}$

*Different letters indicate statistical difference (significance equal to 95%).

Table 5
Mean and standard deviation (log) of bacterial growth (CFU/mL) in biofilm-forming capability assay for Bioglass®, Biosilicate®, and Bio-FP. Negative control: alumina.

Bacteria	Bioglass®	Biosilicato®	Bio-FP	Negative control
A. naeslundii (ATCC 19039)	0 ± 0.00	0 ± 0.00	0 ± 0.00	6.90 ± 0.54
F. nucleatum (ATCC 25586)	0 ± 0.00	0 ± 0.00	0 ± 0.00	8.22 ± 0.76
F. nucleatum (clinical isolate)	0 ± 0.00	0 ± 0.00	0 ± 0.00	8.65 ± 1.13
P. gingivalis (ATCC 33277)	0 ± 0.00	0 ± 0.00	0 ± 0.00	9.26 ± 1.18
P. gingivalis (clinical isolate)	0 ± 0.00	0 ± 0.00	0 ± 0.00	8.15 ± 0.73
P. nigrescens (ATCC 33563)	0 ± 0.00	0 ± 0.00	0 ± 0.00	8.16 ± 0.98
S. sobrinus (ATCC 33478)	0 ± 0.00	0 ± 0.00	0 ± 0.00	7.52 ± 1.12
S. mutans (ATCC 25175)	0 ± 0.00	0 ± 0.00	0 ± 0.00	8.19 ± 1.61
S. mitis (ATCC 49456)	0 ± 0.00	0 ± 0.00	0 ± 0.00	7.90 ± 0.65
L. casei (ATCC 11578)	0 ± 0.00	0 ± 0.00	0 ± 0.00	8.30 ± 1.71
L. casei (clinical isolate)	0 ± 0.00	0 ± 0.00	0 ± 0.00	7.84 ± 1.49

biofilm formation of microorganisms responsible for some oral diseases — setting up an alternative to solve the emergent problem of increasing bacterial resistance.

3.3.3. Direct contact method

The results of the direct contact assay shown in Table 6 reinforce those of the biofilm-forming capability previously demonstrated. Here, it was possible to confirm the high antibacterial effect of the tested

Table 6
Mean and standard deviation (log) of bacterial growth (CFU/mL) in direct contact assay for Bioglass®, Biosilicate®, and Bio-FP. Negative control: alumina.

Bacteria	Initial count	Bioglass®		Biosilicate®		Bio-FP		Negative control	
Time:	0 mim	10 min	60 mim	10 min	60 mim	10 min	60 mim	10 min	60 mim
A. naeslundii (ATCC 19039)	9.5	0 ± 0.0	0 ± 0.0	9.9 ± 0.1	0 ± 0.0	0 ± 0.0	0 ± 0.0	10.0 ± 0.9	10.5 ± 0.8
F. nucleatum (ATCC 25586)	9.5	0 ± 0.0	0 ± 0.0	0 ± 0.0	0 ± 0.0	0 ± 0.0	0 ± 0.0	10.1 ± 0.7	10.1 ± 0.8
F. nucleatum (clinical isolate)	9.5	0 ± 0.0	0 ± 0.0	0 ± 0.0	0 ± 0.0	0 ± 0.0	0 ± 0.0	10.0 ± 0.9	10.1 ± 0.8
P. gingivalis (ATCC 33277)	9.5	0 ± 0.0	0 ± 0.0	0 ± 0.0	0 ± 0.0	0 ± 0.0	0 ± 0.0	9.2 ± 0.6	9.4 ± 0.3
P. gingivalis (clinical isolate)	9.5	0 ± 0.0	0 ± 0.0	0 ± 0.0	0 ± 0.0	0 ± 0.0	0 ± 0.0	9.9 ± 0.7	10.1 ± 0.8
P. nigrescens (ATCC 33563)	9.4	0 ± 0.0	0 ± 0.0	0 ± 0.0	0 ± 0.0	0 ± 0.0	0 ± 0.0	9.0 ± 0.9	9.5 ± 0.6
S. sobrinus (ATCC 33478)	9.3	0 ± 0.0	0 ± 0.0	0 ± 0.0	0 ± 0.0	9.9 ± 0.4	0 ± 0.0	9.7 ± 0.8	9.7 ± 0.5
S. mutans (ATCC 25175)	9.1	0 ± 0.0	0 ± 0.0	10.5 ± 0.1	0 ± 0.0	0 ± 0.0	0 ± 0.0	9.7 ± 0.9	9.8 ± 0.9
S. mitis (ATCC 49456)	9.9	0 ± 0.0	0 ± 0.0	0 ± 0.0	0 ± 0.0	0 ± 0.0	0 ± 0.0	9.7 ± 0.6	10.3 ± 0.5
L. casei (ATCC 11578)	9.5	0 ± 0.0	0 ± 0.0	10.08 ± 0.4	0 ± 0.0	10.1 ± 0.3	10.1 ± 0.5	9.8 ± 0.4	10.1 ± 0.8
L. casei (clinical isolate)	9.5	0 ± 0.0	0 ± 0.0	0 ± 0.0	0 ± 0.0	0 ± 0.0	0 ± 0.0	9.3 ± 0.4	9.4 ± 0.8

materials because the Bioglass® (positive control), Biosilicate®, and Bio-FP practically eliminated all viable cells after only 10 min of contact with the bacteria. On the other hand, we observed a small increase in the number of CFUs in the negative control (Al_2O_3) when comparing the initial count, at zero time, and after 10 and 60 min. Again, this result provides strong evidence that the observed antibacterial effect is exclusive to the materials, and there is no external interference.

In relation to the bacteria evaluated in the direct contact method, we highlight the effect of these materials against *F. nucleatum* (ATCC 25586/clinical isolate) and *P. nigrescens* (ATCC 33563), which presented less susceptibility in the MIC assay. In the case of *E. faecalis* (ATCC 4082), which also demonstrated a higher resistance, and for the other bacteria that form biofilms and were not evaluated by this method, we can expect similar results based on data published by Martins et al. [42] for Biosilicate®. Evaluating the effect of that material against 20 microorganisms, these authors also verified that most of them are eliminated in only 10 min. An exception was found for *S. aureus* (ATCC 6538), which remained alive even after 60 min but with a reduction from 5.3 to 2.6 ± 0.4 CFU/mL.

As shown in Table 6, all bacteria were eliminated in the first 10 min of contact with Bioglass®. In the case of Biosilicate®, after 10 min it was still possible to verify the presence of *S. mutans* (ATCC 25175), *L. casei* (ATCC 11578), and *A. naeslundii* (ATCC 19039), but all bacteria were eliminated by 60 min. For the Bio-FP, viable cells of *S. sobrinus* (ATCC 33478) and also *L. casei* (ATCC 11578) were identified after the first 10 min. At 60 min, only *S. sobrinus* (ATCC 33478) was completely extinct. These data are somewhat discrepant because Biosilicate® and Bio-FP are very similar in composition and structure. During the test, some experimental error may have occurred; however, this possibility does not invalidate most of the results, which are consistent as a whole.

Among the possible mechanisms that may explain the high antibacterial activity observed for the Bioglass®, Biosilicate®, and Bio-FP in this direct contact assay, involving the intimate contact of the bacteria with the material, we can mention the pH increase and the osmotic pressure effect [8,9]. Debris released from the materials in the medium may also have had an influence [10]. To verify the effect of pH, we measured its variation for the tested samples, immersing them in a 0.9% NaCl solution, reproducing the conditions used in the direct contact assay (proportion of 50 mg/mL). As shown in Fig. 10, all samples promoted an increase in pH — Bioglass®, Biosilicate®, and Bio-FP essentially by the release of alkaline species with dissolution, and Al_2O_3 because that compound behaves as a weak base in an aqueous medium, preferentially adsorbing H^+ and, consequently, increasing the pH.

Starting from ~6, the pH reached a value of approximately 11 for Bioglass®, Biosilicate®, and Bio-FP after 10 min, while for alumina the pH was found to be 9.6. The most abrupt change occurred in the first

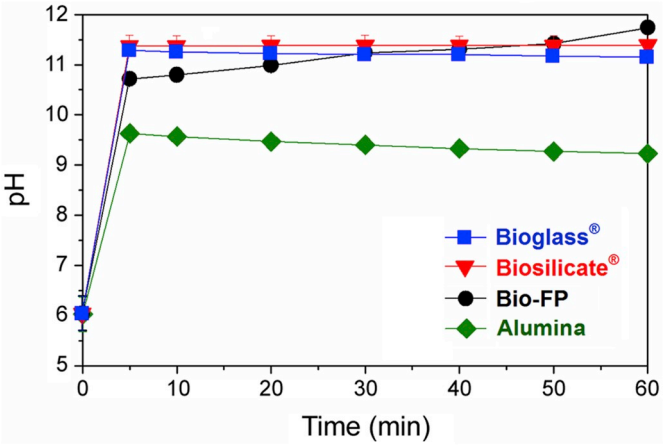

Fig. 10. Variations in pH provided by Bioglass®, Biosilicate®, Bio-FP, and alumina (negative control) as a function of immersion time in 0.9% NaCl solution.

Table 7
Molar concentration of hydroxyl ions related to pH variation.

Time (min)	Alumina	Bioglass®	Biosilicate	Bio-FP
	$[OH^-]$	$[OH^-]$	$[OH^-]$	$[OH^-]$
0	1.071×10^{-8}	1.071×10^{-8}	1.071×10^{-8}	1.071×10^{-8}
5	4.266×10^{-5}	1.905×10^{-3}	2.291×10^{-3}	4.898×10^{-4}
10	3.715×10^{-5}	1.778×10^{-3}	2.291×10^{-3}	5.888×10^{-4}
20	2.951×10^{-5}	1.660×10^{-3}	2.344×10^{-3}	9.120×10^{-4}
30	2.512×10^{-5}	1.585×10^{-3}	2.344×10^{-3}	1.622×10^{-3}
40	2.138×10^{-5}	1.585×10^{-3}	2.344×10^{-3}	1.905×10^{-3}
50	1.862×10^{-5}	1.479×10^{-3}	2.344×10^{-3}	2.455×10^{-3}
60	1.698×10^{-5}	1.413×10^{-3}	2.399×10^{-3}	5.129×10^{-3}

10 min, with only a small pH variation up to 60 min. Therefore, the increase in pH seems to play a role in the antibacterial effect of these materials, even with a variation of only ~1.4, which was observed between the tested samples and the negative control. It is important to note that the pH is presented in a log scale, thus the change in hydroxyl ions (OH^-) in the medium related to the pH variation corresponds to two orders of magnitude, as shown in Table 7 — results that potentially helping to explain the data shown in Table 6. For tested samples, the number of viable cells zeroed for almost all bacteria after 10 min, whereas in the negative control, this value increased. Thus, we can relate the antibacterial effect observed to the increase in pH, but it is important to mention the release of some ions, such as Ca^{2+}, which can cause the death of bacteria promoting the depolarization of their cell membrane, as a consequence of the high ion concentration at the interface between the materials (particle) and bacteria (cell membrane) [68]. The release of silica is also a factor that may contribute to antibacterial activity. According to Waltimo et al. [62], because silica solutions themselves have been suggested for food disinfection [69], an ideal antimicrobial agent would combine high silica delivery, high pH, and a high alkaline buffer capacity.

As mentioned previously, the set of samples Bio-FP(Ag), Bio-FP (Mg), Bio-FP(Sr), Bio-FP(Zn), and Bio-FP(Ga) were not evaluated by this method of direct contact because the Bio-FP already exhibited satisfactory results for the purpose of this study, with an effect comparable to the reference materials, Bioglass® and Biosilicate®. It is important to note that in addition to the good antibacterial activity determined by the MIC (see Tables 2–4), doped samples may also have important additional properties that could be investigated, such as osteogenic and anti-osteoporotic characteristics, in the case of those containing Sr and Ga, for example. Obviously, these investigations should be accompanied by a study involving their degradability, ion release profile, and cytotoxicity.

4. Summary and conclusions

Bioactive ceramics of the $SiO_2-CaO-Na_2O-P_2O_5$ system containing up to 3 mol% of Ag, Mg, Sr, Zn, and Ga were synthesized using a solid-state reaction. All the materials showed good *in vitro* bioactivity, with HCA layer formation after 24 h *in vitro* for samples doped with 0.5%, and after 120 h for those with 1 and 3 mol%. Although the bioactive response decreased for high dopant concentrations, the doped samples may have important additional properties, and thus warrant future studies considering the importance of verifying their degradability rates, ion release profile, and cytotoxicity.

In testing the new ICG-TC04 bioactivity method (so far only tested for glasses), we observed that it is also effective for evaluating the *in vitro* bioactivity of crystalline materials. The method proved to be easy to implement and rapid, besides requiring a small amount of sample. However, for crystalline samples, particularly those with intense XRD peaks at around 26 and 32° (2θ), the same region where the hydroxyapatite peaks are located, the analysis needs to be performed carefully.

The antibacterial activity of the resulting materials was evaluated against 23 potentially pathogenic anaerobic and aerobic/microaerophilic bacteria related to caries and endodontic infections. All samples were tested in parallel with the reference materials Bioglass® and Biosilicate®, and their expressive antibacterial activity was evident. Although the increase of the Ag, Mg, Sr, Zn, and Ga content from 0.5 to 3% did not have a significant effect on the selected bacteria, the presence of Ag was clearly sufficient to amplify the activity spectrum within the concentration range of 0.5–24 mg/mL, defined by MIC values in the agar dilution assay. In the biofilm-forming capability and direct contact assays, in which the samples were intimately in contact with the bacteria, 10 min was sufficient to eliminate almost all bacteria evaluated. The same effect may be observed for shorter times, but this supposition requires further investigation. In any case, because the tested materials present a broad spectrum of activity, even at a low concentration and being extremely effective in direct contact, they could be tested for different applications, such as oral bone defect treatments, root canal disinfection, and dental prophylaxis procedures.

Acknowledgments

We are grateful to the Brazilian agencies CAPES, CNPq, and FAPESP (CEPID, grant #2013/07793-6), for generous funding, and for the scholarships granted to R. L. Siqueira (PNPD/CAPES, #2018/1759041) and P. F. S. Alves (FAPESP, #2014/07483-0). We also thank biologist Danielli F. Pinto for their valuable discussions and suggestions.

References

[1] L.L. Hench, Bioceramics: from concept to clinic, J. Am. Ceram. Soc. 74 (1991) 1487–1510, https://doi.org/10.1111/j.1151-2916.1991.tb07132.x.
[2] L.L. Hench, The story of Bioglass®, J. Mater. Sci. Mater. Med. 17 (2006) 967–978, https://doi.org/10.1007/s10856-006-0432-z.
[3] A.J. Salinas, M. Vallet-Regí, Bioactive ceramics: from bone grafts to tissue engineering, RSC Adv. 3 (2013) 11116–11131, https://doi.org/10.1039/c3ra00166k.
[4] V. Miguez-Pacheco, L.L. Hench, A.R. Boccaccini, Bioactive glasses beyond bone and teeth: emerging applications in contact with soft tissues, Acta Biomater. 13 (2015) 1–15, https://doi.org/10.1016/j.actbio.2014.11.004.
[5] A. Hoppe, N.S. Güldal, A.R. Boccaccini, A review of the biological response to ionic dissolution products from bioactive glasses and glass-ceramics, Biomaterials 32 (2011) 2757–2774, https://doi.org/10.1016/j.biomaterials.2011.01.004.
[6] S.M. Rabiee, N. Nazparvar, M. Azizian, D. Vashaee, L. Tayebi, Effect of ion substitution on properties of bioactive glasses: a review, Ceram. Int. 41 (2015) 7241–7251, https://doi.org/10.1016/j.ceramint.2015.02.140.
[7] L. Drago, C. Vassena, S. Fenu, E. De Vecchi, V. Signori, R. De Francesco, C.L. Romanò, *In vitro* antibiofilm activity of bioactive glass S53P4, Future Microbiol. 9 (2014) 593–601, https://doi.org/10.2217/fmb.14.20.
[8] P. Stoor, E. Söderling, J.I. Salonen, Antibacterial effects of a bioactive glass paste on oral microorganisms, Acta Odontol. Scand. 56 (1998) 161–165, https://doi.org/10.1080/000163598422901.
[9] I. Allan, H. Newman, M. Wilson, Antibacterial activity of particulate Bioglass® against supra- and subgingival bacteria, Biomaterials 22 (2001) 1683–1687, https://doi.org/10.1016/S0142-9612(00)00330-6.
[10] S. Hu, J. Chang, M. Liu, C. Ning, Study on antibacterial effect of 45S5 Bioglass®, J. Mater. Sci. Mater. Med. 20 (2009) 281–286, https://doi.org/10.1007/s10856-008-3564-5.
[11] E. Munukka, O. Leppäranta, M. Korkeamäki, M. Vaahtio, T. Peltola, D. Zhang, L. Hupa, H. Ylänen, J.I. Salonen, M.K. Viljanen, E. Eerola, Bactericidal effects of bioactive glasses on clinically important aerobic bacteria, J. Mater. Sci. Mater. Med. 19 (2008) 27–32, https://doi.org/10.1007/s10856-007-3143-1.
[12] S. Salehi, H.B. Davis, J.L. Ferracane, J.C. Mitchell, Sol-gel-derived bioactive glasses demonstrate antimicrobial effects on common oral bacteria, Am. J. Dent. 28 (2015) 111–115.
[13] N.A.P. Van Gestel, J. Geurts, D.J.W. Hulsen, B. Van Rietbergen, S. Hofmann, J.J. Arts, Clinical applications of S53P4 bioactive glass in bone healing and osteomyelitic treatment: a literature review, BioMed Res. Int. 2015 (2015) 1–12, https://doi.org/10.1155/2015/684826.
[14] J.-C. Aurégan, T. Bégué, Bioactive glass for long bone infection: a systematic review, Injury 46 (2015) S3–S7, https://doi.org/10.1016/S0020-1383(15)30048-6.
[15] J. Kankare, N.C. Lindfors, Reconstruction of vertebral bone defects using an expandable replacement device and bioactive glass S53P4 in the treatment of vertebral osteomyelitis: three patients and three pathogens, Scand. J. Surg. 105 (2016) 248–253, https://doi.org/10.1177/1457496915626834.
[16] J.L. Clement, P.S. Jarrett, Antibacterial silver, Met. Based. Drugs 1 (1994) 467–482, https://doi.org/10.1155/MBD.1994.467.
[17] K. Mijnendonckx, N. Leys, J. Mahillon, S. Silver, R. Van Houdt, Antimicrobial silver: uses, toxicity and potential for resistance, Biometals 26 (2013) 609–621, https://doi.org/10.1007/s10534-013-9645-z.
[18] M. Bellantone, H.D. Williams, L.L. Hench, Broad-spectrum bactericidal activity of Ag_2O-doped bioactive glass, Antimicrob. Agents Chemother. 46 (2002) 1940–1945, https://doi.org/10.1128/AAC.46.6.1940-1945.2002.
[19] S. Di Nunzio, C. Vitale Brovarone, S. Spriano, D. Milanese, E. Verné, V. Bergo, G. Maina, P. Spinelli, Silver containing bioactive glasses prepared by molten salt ion-exchange, J. Eur. Ceram. Soc. 24 (2004) 2935–2942, https://doi.org/10.1016/j.jeurceramsoc.2003.11.010.
[20] A. Mishra, J. Rocherullé, J. Massera, Ag-doped phosphate bioactive glasses: thermal, structural and in-vitro dissolution properties, Biomed. Glasses 2 (2016) 38–48, https://doi.org/10.1515/bglass-2016-0005.
[21] J.J. Blaker, S.N. Nazhat, A.R. Boccaccini, Development and characterisation of silver-doped bioactive glass-coated sutures for tissue engineering and wound healing applications, Biomaterials 25 (2004) 1319–1329, https://doi.org/10.1016/j.biomaterials.2003.08.007.
[22] G. Hu, L. Xiao, P. Tong, D. Bi, H. Wang, H. Ma, G. Zhu, H. Liu, Antibacterial hemostatic dressings with nanoporous bioglass containing silver, Int. J. Nanomed. 7 (2012) 2613–2620, https://doi.org/10.2147/IJN.S31081.
[23] Y. Kaneko, M. Thoendel, O. Olakanmi, B.E. Britigan, P.K. Singh, The transition metal gallium disrupts *Pseudomonas aeruginosa* iron metabolism and has antimicrobial and antibiofilm activity, J. Clin. Invest. 117 (2007) 877–888, https://doi.org/10.1172/JCI30783.
[24] S.P. Valappil, D. Ready, E.A. Abou Neel, D.M. Pickup, W. Chrzanowski, L.A. O'Dell, R.J. Newport, M.E. Smith, M. Wilson, J.C. Knowles, Antimicrobial gallium-doped phosphate-based glasses, Adv. Funct. Mater. 18 (2008) 732–741, https://doi.org/10.1002/adfm.200700931.
[25] P. Melnikov, A. Malzac, M. de B. Coelho, Gallium and bone pathology, Acta Ortopédica Bras. 16 (2008) 54–57, https://doi.org/10.1590/S1413-78522008000100011.
[26] E. Verron, J.M. Bouler, J.C. Scimeca, Gallium as a potential candidate for treatment of osteoporosis, Drug Discov. Today 17 (2012) 1127–1132, https://doi.org/10.1016/j.drudis.2012.06.007.
[27] P.J. Marie, Strontium as therapy for osteoporosis, Curr. Opin. Pharmacol. 5 (2005) 633–636, https://doi.org/10.1016/j.coph.2005.05.005.
[28] P.R. Rizzoli, Osteoporosis: non-hormonal treatment, Climacteric 10 (2007) 74–78, https://doi.org/10.1080/13697130701600815.
[29] E. Gentleman, Y.C. Fredholm, G. Jell, N. Lotfibakhshaiesh, M.D. O'Donnell, R.G. Hill, M.M. Stevens, The effects of strontium-substituted bioactive glasses on osteoblasts and osteoclasts *in vitro*, Biomaterials 31 (2010) 3949–3956, https://doi.org/10.1016/j.biomaterials.2010.01.121.
[30] A.L.B. Maçon, T.B. Kim, E.M. Valliant, K. Goetschius, R.K. Brow, D.E. Day, A. Hoppe, A.R. Boccaccini, I.Y. Kim, C. Ohtsuki, T. Kokubo, A. Osaka, M. Vallet-Regí, D. Arcos, L. Fraile, A.J. Salinas, A.V. Teixeira, Y. Vueva, R.M. Almeida, M. Miola, C. Vitale-Brovarone, E. Verné, W. Höland, J.R. Jones, A unified *in vitro* evaluation for apatite-forming ability of bioactive glasses and their variants, J. Mater. Sci. Mater. Med. 26 (2015) 115–125, https://doi.org/10.1007/s10856-015-5403-9.
[31] R.L. Siqueira, E.D. Zanotto, Facile route to obtain a highly bioactive $SiO_2-CaO-Na_2O-P_2O_5$ crystalline powder, Mater. Sci. Eng. C 31 (2011) 1791–1799, https://doi.org/10.1016/j.msec.2011.08.013.
[32] R.L. Siqueira, J.H. Alano, O. Peitl, E.D. Zanotto, GlassPanacea: an efficient software for the formulation of ceramic materials, Quim. Nova 41 (2018) 446–450, https://doi.org/10.21577/0100-4042.20170196.
[33] R.L. Siqueira, J.H. Alano, O. Peitl, E.D. Zanotto, GlassPanacea: a user-friendly free software tool for the formulation of glasses, glass-ceramics, and ceramics, Am. Ceram. Soc. Bull. 96 (2017).
[34] C. Ravagnani, Biosilicate for Oral Health Promotion, Master of Science and Materials Engineering (Supervisor E.D. Zanotto) Universidade Federal de São Carlos, 2003.
[35] E.D. Zanotto, C. Ravagnani, O. Peitl, H. Panzeri, E.H.G. Lara, Process and Compositions for Preparing Particulate, Bioactive or Resorbable Biosilicates for Use in the Treatment of Oral Ailments, (2004) Patent WO/2004/074199 https://www.surechembl.org/document/KR-20060010719-A.
[36] M.C. Crovace, M.T. Souza, C.R. Chinaglia, O. Peitl, E.D. Zanotto, Biosilicate® — a multipurpose, highly bioactive glass-ceramic. *In vitro, in vivo* and clinical trials, J. Non-Cryst. Solids 432 (2016) 90–110, https://doi.org/10.1016/j.jnoncrysol.2015.03.022.
[37] R.L. Siqueira, E.D. Zanotto, Biosilicate®: historical of a highly bioactive brazilian glass-ceramic, Quim. Nova 34 (2011) 1231–1241, https://doi.org/10.1590/S0100-40422011000700023.
[38] S. Brunauer, P.H. Emmett, E. Teller, Adsorption of gases in multimolecular layers, J. Am. Chem. Soc. 60 (1938) 309–319, https://doi.org/10.1021/ja01269a023.
[39] ISO 23317: 2007, Implants for Surgery — In Vitro Evaluation for Apatite-Forming Ability of Implant Materials, Geneva Int. Organ. Stand., 2007.
[40] T. Kokubo, H. Takadama, How useful is SBF in predicting *in vivo* bone bioactivity? Biomaterials 27 (2006) 2907–2915, https://doi.org/10.1016/j.biomaterials.2006.01.017.
[41] C. Tirapelli, H. Panzeri, E.H.G. Lara, R.G. Soares, O. Peitl, E.D. Zanotto, The effect of a novel crystallised bioactive glass-ceramic powder on dentine hypersensitivity: a long-term clinical study, J. Oral Rehabil. 38 (2011) 253–262, https://doi.org/10.1111/j.1365-2842.2010.02157.x.
[42] C.H.G. Martins, T.C. Carvalho, M.G.M. Souza, C. Ravagnani, O. Peitl, E.D. Zanotto, H. Panzeri, L.A. Casemiro, Assessment of antimicrobial effect of Biosilicate® against anaerobic, microaerophilic and facultative anaerobic microorganisms, J. Mater. Sci. Mater. Med. 22 (2011) 1439–1446, https://doi.org/10.1007/s10856-011-4330-7.
[43] J.H. Jorgensen, J.D. Turnidge, Susceptibility test methods: dilution and disk

diffusion methods, in: J. Jorgensen, M. Pfaller, K. Carroll, G. Funke, M. Landry, S. Richter, D. Warnock (Eds.), Man. Clin. Microbiol, eleventh ed., ASM Press, Washington, 2015, pp. 1253–1273.
[44] J.J. Harrison, R.J. Turner, H. Ceri, High-throughput metal susceptibility testing of microbial biofilms, BMC Microbiol. 5 (2005) 1–11, https://doi.org/10.1186/1471-2180-5-53.
[45] R.L. Siqueira, N. Maurmann, D. Burguêz, D.P. Pereira, A.N.S. Rastelli, O. Peitl, P. Pranke, E.D. Zanotto, Bioactive gel-glasses with distinctly different compositions: bioactivity, viability of stem cells and antibiofilm effect against *Streptococcus mutans*, Mater. Sci. Eng. C 76 (2017) 233–241, https://doi.org/10.1016/j.msec.2017.03.056.
[46] G.K. Moir, F.P. Glasser, Phase equilibria in the system $Na_2SiO_3-CaSiO_3$, Phys. Chem. Glasses 15 (1974) 6–11.
[47] G.K. Moir, F.P. Glasser, Solid solutions and phase equilibria in the systems $Na_2SiO_3-SrSiO_3$ and $Na_2SiO_3-CaSiO_3-SrSiO_3$, Trans. J. Br. Ceram. Soc. 73 (1974) 199–206.
[48] D.R. Lide, Handbook of Chemistry and Physics, eighty seventh ed., CRC Press, Boca Raton, 2007.
[49] P. Atkins, J. Paula, Physical Chemistry, ninth ed., W. H. Freeman and Company, New York, 2010.
[50] O. Kubaschewski, C.B. Alcock, P.J. Spencer, Materials Thermochemistry, sixth ed., Pergamon Press, New York, 1993.
[51] O. Peitl, E.D. Zanotto, L.L. Hench, Highly bioactive $P_2O_5-Na_2O-CaO-SiO_2$ glass-ceramics, J. Non-Cryst. Solids 292 (2001) 115–126, https://doi.org/10.1016/S0022-3093(01)00822-5.
[52] E.R. Lippincott, A. Van Valkenburg, C.E. Weir, E.N. Bunting, Infrared studies on polymorphs of silicon dioxide and germanium dioxide, J. Res. Natl. Bur. Stand. (1934) 61 (1958) 61–70, https://doi.org/10.6028/jres.061.009.
[53] W. Jastrzębski, M. Sitarz, M. Rokita, K. Bułat, Infrared spectroscopy of different phosphates structures, Spectrochim. Acta Part A Mol. Biomol. Spectrosc. 79 (2011) 722–727, https://doi.org/10.1016/j.saa.2010.08.044.
[54] M. Šupová, Substituted hydroxyapatites for biomedical applications: a review, Ceram. Int. 41 (2015) 9203–9231, https://doi.org/10.1016/j.ceramint.2015.03.316.
[55] W.K. Jung, H.C. Koo, K.W. Kim, S. Shin, S.H. Kim, Y.H. Park, Antibacterial activity and mechanism of action of the silver ion in *Staphylococcus aureus* and *Escherichia coli*, Appl. Environ. Microbiol. 74 (2008) 2171–2178, https://doi.org/10.1128/AEM.02001-07.
[56] R. Sahdev, T.I. Ansari, S.M. Higham, S.P. Valappil, Potential use of gallium-doped phosphate-based glass material for periodontitis treatment, J. Biomater. Appl. 30 (2015) 85–92, https://doi.org/10.1177/0885328215571952.
[57] M. Riaz, R. Zia, F. Saleemi, H. Ikram, F. Bashir, *In vitro* antimicrobial activity of ZnO based glass-ceramics against pathogenic bacteria, J. Mater. Sci. Mater. Med. 26 (2015) 1–12, https://doi.org/10.1007/s10856-015-5603-3.
[58] L. Esteban-Tejeda, C. Prado, B. Cabal, J. Sanz, R. Torrecillas, J.S. Moya, Antibacterial and antifungal activity of ZnO containing glasses, PLoS One 10 (2015) 1–17, https://doi.org/10.1371/journal.pone.0132709.
[59] M. Ottomeyer, A. Mohammadkah, D. Day, D. Westenberg, Broad-spectrum antibacterial characteristics of four novel borate-based bioactive glasses, Adv. Microbiol. 6 (2016) 776–787, https://doi.org/10.4236/aim.2016.610076.
[60] P. Balasubramanian, T. Büttner, V. Miguez-Pacheco, A.R. Boccaccini, Boron-containing bioactive glasses in bone and soft tissue engineering, J. Eur. Ceram. Soc. 38 (2018) 855–869, https://doi.org/10.1016/j.jeurceramsoc.2017.11.001.
[61] M.F. Gorriti, J.M.P. López, A.R. Boccaccini, C. Audisio, A.A. Gorustovich, *In vitro* study of the antibacterial activity of bioactive glass-ceramic scaffolds, Adv. Eng. Mater. 11 (2009) B67–B70, https://doi.org/10.1002/adem.200900081.
[62] T. Waltimo, T.J. Brunner, M. Vollenweider, W.J. Stark, M. Zehnder, Antimicrobial effect of nanometric bioactive glass 45S5, J. Dent. Res. 86 (2007) 754–757, https://doi.org/10.1177/154405910708600813.
[63] P. Saravanapavan, J.E. Gough, J.R. Jones, L.L. Hench, Antimicrobial macroporous gel-glasses: dissolution and cytotoxicity, Key Eng. Mater. 254–256 (2004) 1087–1090, https://doi.org/10.4028/www.scientific.net/KEM.254-256.1087.
[64] G. Sundqvist, D. Figdor, S. Persson, U. Sjögren, Microbiologic analysis of teeth with failed endodontic treatment and the outcome of conservative re-treatment, Oral Surg. Oral Med. Oral Pathol. Oral Radiol. Endod. 85 (1998) 86–93, https://doi.org/10.1016/S1079-2104(98)90404-8.
[65] H.H. Hancock, A. Sigurdsson, M. Trope, J. Moiseiwitsch, Bacteria isolated after unsuccessful endodontic treatment in a North American population, Oral Surg. Oral Med. Oral Pathol. Oral Radiol. Endod. 91 (2001) 579–586, https://doi.org/10.1067/moe.2001.113587.
[66] Ll Narayanan, C. Vaishnavi, Endodontic microbiology, J. Conserv. Dent. 13 (2010) 233–239, https://doi.org/10.4103/0972-0707.73386.
[67] P.D. Marsh, Dental plaque: biological significance of a biofilm and community lifestyle, J. Clin. Periodontol. 32 (2005) 7–15, https://doi.org/10.1111/j.1600-051X.2005.00790.x.
[68] J.S. Moya, L. Esteban-Tejeda, C. Pecharromán, S.R.H. Mello-Castanho, A.C. Da Silva, F. Malpartida, Glass powders with a high content of calcium oxide: a step towards a “green” universal biocide, Adv. Eng. Mater. 13 (2011) B256–B260, https://doi.org/10.1002/adem.201080133.
[69] G.H. Weber, J.K. O'Brien, F.G. Bender, Control of *Escherichia coli* O157:H7 with sodium metasilicate, J. Food Protect. 67 (2004) 1501–1506, https://doi.org/10.4315/0362-028X-67.7.1501.